

AD-A072 302 OCEAN SCIENCE AND ENGINEERING INC WASHINGTON D C
FLOATING OBJECT RECOVERY STUDY.(U)
AUG 70 R J HELGESON
11-2003

F/G 8/10

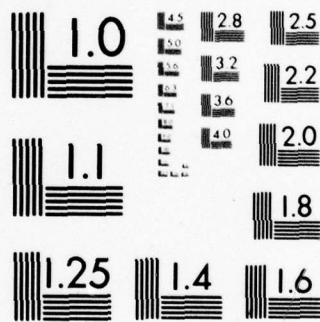
N00014-69-C-0256
NL

UNCLASSIFIED

1 OF 1
AD
A072 0.



END
DATE
FILMED
9-79
DDC



MICROCOPY RESOLUTION TEST CHART
NATIONAL BUREAU OF STANDARDS-1963-A

*Advised
4/26/79*

File

OCT 1970

①
JG
D.C.P.
File Contract

ADA 072302

LEVEL III

"FLOATING OBJECT RECOVERY STUDY"

Final Report

August 31, 1970

**DDC
REFILING
AUG 6 1979
C**

Sponsored by

Office of Naval Research

Contract Number N00014-69-C-0256 P001

Contracting Authority Identification Number

NR 291-026/8+13-69 Code 485

Reproduction in whole or in part is permitted for any purpose of the United States Government

DDC FILE COPY

OCEAN SCIENCE AND ENGINEERING INC.

This document has been approved for public release and sale; its distribution is unlimited.

OCT 1970

79 07 12 085

DOCUMENT CONTROL DATA - R & D

(Security classification of title, body of abstract and indexing annotation must be entered when the overall report is classified)

1. ORIGINATING ACTIVITY (Corporate author) Ocean Science and Engineering, Incorporated	2a. REPORT SECURITY CLASSIFICATION Unclassified
	2b. GROUP N. A.

3. REPORT TITLE

FLOATING OBJECT RECOVERY STUDY

4. DESCRIPTIVE NOTES (Type of report and inclusive dates)
FINAL

5. AUTHOR(S) (First name, middle initial, last name)

RICHARD J. HELGESON

6. REPORT DATE August 31, 1970	7a. TOTAL NO. OF PAGES 46	7b. NO. OF REFS 12
8a. CONTRACT OR GRANT NO. N00014-69-C-0256	8b. ORIGINATOR'S REPORT NUMBER(S) 11-2003	
b. PROJECT NO. <i>Contract file</i>	8c. OTHER REPORT NO(S) (Any other numbers that may be assigned this report) N. A.	
c.		
d.		

10. DISTRIBUTION STATEMENT
Reproduction in whole or part is permitted for any purpose of the United States Government.

11. SUPPLEMENTARY NOTES N. A.	12. SPONSORING MILITARY ACTIVITY Office of Naval Research
---	---

13. ABSTRACT

A study was conducted to determine a method to recover floating objects from the surface of the ocean. Model test tank investigations conducted at Stevens Institute of generating a localized flow field which would refract waves were investigated for a possible practical application. Several methods of generating a localized flow field in the open ocean were investigated. The flow field could attenuate wave energies in an area which could possibly facilitate the recovery of floating objects from the ocean surface.

⑥ Floating Object Recovery Study

⑫ 53p.

⑨ Final Report
August 31, 1970

DDC
RECEIVED
AUG 6 1971
C

⑪ 31 Aug 70

Ocean Science and Engineering, Inc.

Washington, D.C.

⑩ Richard J. Helgeson

⑭ 11-2003

Sponsored by

Office of Naval Research

Contract Number ^⑮ ~~NO0014-69-C-0256~~ P001

Contracting Authority Identification Number 21

NR 291-026/8-13-69 Code 485

Reproduction in whole or in part is permitted for any purpose of the United States Government

✓ 387058

This document has been approved for public release and sale; its distribution is unlimited.

LB

TABLE OF CONTENTS

<u>Part</u>	<u>Title</u>	<u>Page</u>
1.	Introduction	1
2.	Refraction	3
3.	Surf and Swell Forecasting	4
4.	Surface Wave Refraction by a Flow Field	6
5.	Diffraction and Superposition	8
6.	Ocean Wave Directional Spectrum	15
7.	Oceanographic Research Ship	15
8.	Calculations	17
9.	Energy Required to Generate a Refractive Flow Field	17
10.	Expected Attenuation in a Fully Developed Wind Driven Sea	19
11.	Time Estimate of Refractive Effect Persistence	21
12.	General Properties of Refractive Flow Fields	23
13.	Application of Refractive Flow Field to Oceanographic Operations	24
14.	Recommendations	31

Bibliography

Appendix. Motions of Oceanographic Research Ship in Irregular Head Seas

Accession For	
NTIS	GRA&I
DDC	TAB
Unannounced	
Justification	
By <i>file</i>	
Distribution/	
Availability Codes	
Dist.	Availand/or special
<i>A</i>	

LIST OF ILLUSTRATIONS

<u>Figure</u>	<u>Title</u>	<u>Page</u>
1.	Underwater Acoustic Propagation Paths with Convex Propagation Velocity Profile	5
2.	Refraction Diagram Showing Destructive Waves at Long Beach	5
3.	Longitudinal Velocity Distribution in Grid Wake (Savitsky, 1970)	9
4.	Calm Patch Produced by a Sharply Peaked Flow Field	11
5.	Diffraction of Waves at Breakwater Gap (Johnson, 1952)	12
6.	Computed Versus Measured Crest Height (Savitsky, 1970)	13
7.	Computed Versus Measured Crest Height (Savitsky, 1970)	14
8.	Final Directional Wave Energy Spectrum from SWOP (Cote et al., 1960)	16
9.	Computed Wave Refraction Diagram (Savitsky, 1970)	20
10.	Envelope of Wave Height at Wave Probes Moving in Wake of 2-Dimensional Grid	22
11.	Propeller Wash Utilization with Flow Along Flaps	27
12.	Propeller Wash Utilization with Side Net Drogues	28
13.	Propeller Wash Utilization with Suspended Net Drogue	29
14.	Flow Field Generated by a Towed Grid	30

1. Introduction

Recovering objects by ships from the surface of the ocean is made difficult because of the difference in the dynamic response to surface waves of the object and the ship. This difference in response often results in large relative displacements and velocities which can induce unexpectedly large forces in the recovery system and the object being recovered.

Motion compensating recovery systems have been designed in such a way that their dynamic response can be adjusted during the recovery operation. For instance: immediately after the recovery line is secured to the object, a "constant force" recovery system is desirable because large relative displacements will continue to occur until the object is entirely clear of the water. When the object is swung over the deck, however, a "constant displacement" system is desirable to prevent the object from attaining a high velocity with respect to the ship. The two modes of optimum operation are mutually exclusive and a compensating recovery system must be able to operate in both modes. In general, these systems are complex, expensive, and limited with respect to versatility in the types of objects which can be recovered. They are usually designed to recover one particular object.

Another approach to the recovery problem might be an attempt to match the dynamic response of the ship and the object. This method, even though perfectly executed, could only result in partial success due to the statistically random nature of a fully developed wind driven sea. Its usefulness would also be limited to recovery of objects of similar dynamic responses.

The other main approach to simplifying ship load handling has been

to prevent the waves from reaching the operational area. The best example of this is the use of protected harbors for cargo transfer. Recovery of small boats in the lee of a mother ship utilizes the same principle. This technique stops the progress of a wave by either reflecting the wave or causing it to break and dissipate its energy. Reflection and dissipation require large, massive objects on the same size scale as the wave itself.

Pneumatic and hydraulic breakwaters can be used to reduce the height of a wave as it passes through the breakwater. They work on the principle that a wave which is near breaking can be caused to break if its velocity is increased. A water flow opposite to the direction of wave advance will increase the wave speed relative to the water and cause the wave to break. Hydraulic breakwaters produce a water flow by pumping water directly against the wave approach direction. Pneumatic breakwaters produce a linear bubble screen parallel to the wave crest. This bubble screen in turn produces an upward flow of water which diverges at the surface into two horizontal flows. It is the horizontal flow which causes the wave to break.

These systems are limited in that they only reduce the wave energy and are most effective on small waves. They also require large fluid conductors and relatively large sources of fluid power.

One last technique which has historically been used to calm the ocean's surface is to place oil onto the water. The oil film has the effect of locally increasing the surface tension of the water which reduces the amplitude of small waves and prevents the formation of wind driven spray.

The effect of oil on long period waves which affect the operation of ships is negligible.

In all, the above-mentioned methods of reducing wave amplitude, some physical property of the wave is changed in such a way as to cause the wave to lose energy and provide a zone of wave energy less than that of the surrounding sea surface.

Two main points can be inferred from the operation of existing wave reduction techniques. First, that they can all be explained in terms of the physical properties of surface wave propagation, and secondly, that all the above methods rely on reflecting or attenuating waves to form a low wave energy zone.

2. Refraction

The physical principle of wave refraction causes a wave to "change its direction" as it passes through the refractive medium. It is the principle which governs the design of lenses in optical systems and is basic to the explanation of propagation paths in underwater acoustics as developed in Bartberger (1965). Wave refraction is caused by the wave passing through a region of non-constant propagation velocity. This region may have discontinuous boundaries as in the case of an optical lens or it may consist of a continuous propagation speed gradient such as that which forms the SOFAR acoustic channel in the ocean.

Briefly stated, the law of refraction states:

1. The curvature of a wave ray is equal to the logarithmic velocity gradient along the wave front, and
2. The ray bends toward the direction of lower velocity.

A ray as referred to here is a line continuously perpendicular to an individual wave front which is a line of constant energy propagation phase. In acoustics, this wave front is the sound pressure fluctuation produced by a pinger, in optics it is the electromagnetic activity of a photon, and in surface waves it is a wave crest.

Fig. 1 shows a series of acoustic rays refracted by the sound velocity gradient shown on the right. It is interesting to note the "shadow zone," a region of the ocean into which no acoustic waves are propagated under these conditions. The refraction diagram predicts a region of no acoustic energy even though the acoustic projector may be pointed in that direction, however, the region is not entirely without insonification as predicted. When combined with other wave propagation phenomena such as reverberation and diffraction, the law of refraction can be used to predict the acoustic energy level produced by a projector in the ocean surrounding it.

The problem then is to apply the principle of wave refraction to surface waves on the ocean in order to produce an area of diminished wave energy in which a surface vessel can operate. In order to do this, we must produce a region in the ocean where the wave propagation velocity is different from that surrounding it, and for a truly representative analysis we must take into consideration other wave propagation principles which will modify the result. These principles must then be applied to the unique wave composition of a fully developed, wind driven sea.

3. Surf and Swell Forecasting

During the 1940's, the principle of wave refraction was widely employed

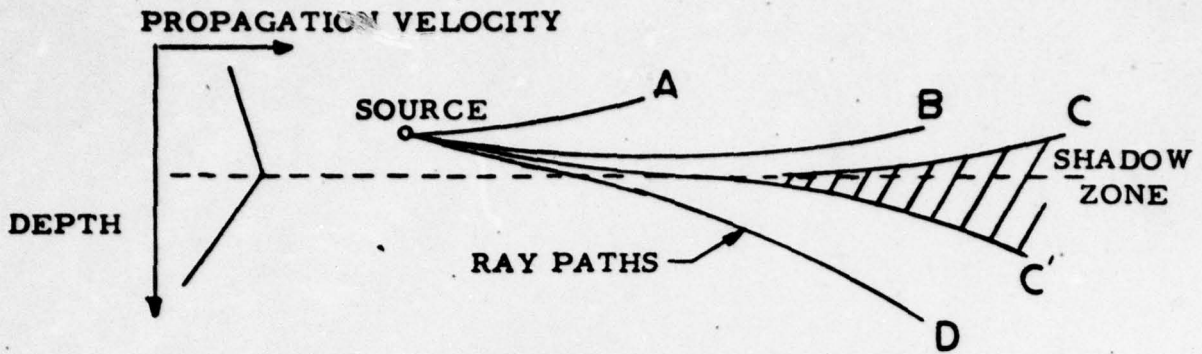


FIGURE 1, UNDERWATER ACOUSTIC PROPAGATION PATHS WITH CONVEX PROPAGATION VELOCITY PROFILE BARTBERGER (1965)

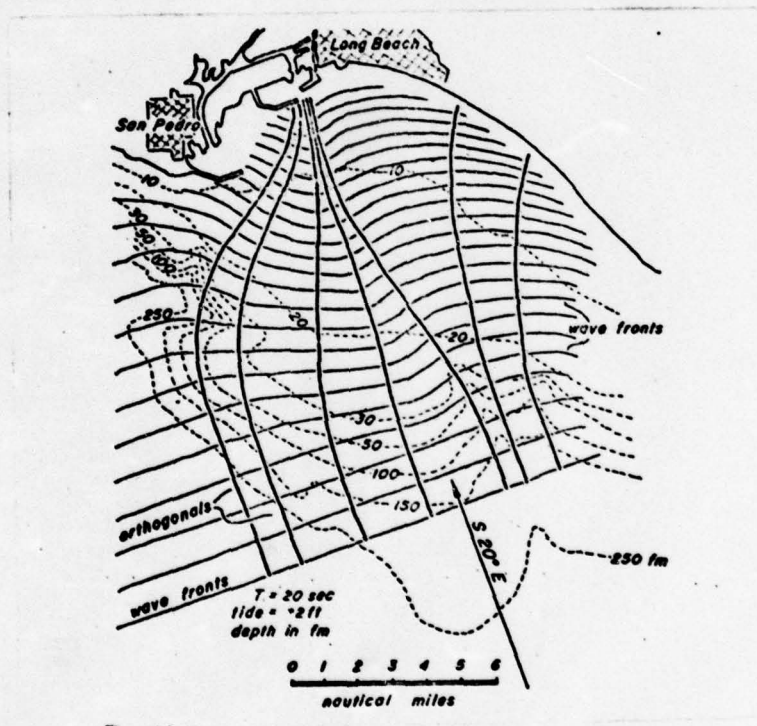


FIGURE 2, REFRACTION DIAGRAM FOR DESTRUCTIVE WAVES AT LONG BEACH, CALIFORNIA SHOWING HOW UNDERWATER TOPOGRAPHY SEVERAL HUNDRED FEET DEEP AND A DOZEN MILES OFFSHORE FOCUSED WAVE ENERGY ON THE BREAK-WATER, BASCUM (1964) FROM O'BRIEN (1947)

to predict the path of waves as they entered shallow water. That is, of course, shallow in the sense that the wave's propagation velocity is determined by the water depth or a depth of about half the wave length. As the wave progresses into shallow water, its propagation speed, amplitude, and wavelength change, while the wave period, measured at any geographical point along the ray, will remain constant.

Fig. 2 shows the effect of local submarine topography on waves approaching Long Beach, California. The concentration of wave rays at the breakwater tip had unexpected results during the period April 20-24, 1930 when large breakers damaged the breakwater. A few miles to the north and south no unusual wave activity was noticed. Seventeen years later, M. P. O'Brien explained this unusual phenomenon by showing that waves from a storm in the South Pacific had been refracted by the submarine topography and their energy was concentrated on a short segment of the breakwater.

4. Surface Wave Refraction by a Flow Field

In the open ocean, the depth is too great to effect propagation so another means must be employed to change the propagation velocity and use the principle of refraction to advantage. This has been shown to be possible by causing a localized ocean current (or flow field) where a region of the ocean's surface water is set into motion. As waves enter this flow field, their propagation velocity is changed and refraction takes place.

All material in this section is based on recent work by Dr. Daniel Savitsky and his report on "Interaction Between Gravity Waves and Finite

Turbulent Flow Fields" (1970) prepared for the Office of Naval Reserach, Contract No. NR-062-254.

The primary difference between topographically induced refraction and flow field induced refraction is that topographical refraction is a scalar mechanism whereas flow field refraction is a vector mechanism. That is, the wave propagation velocity at a specific point in topographical refraction is independent of wave approach angle. A wave approaching from the right will be influenced by the topography in the same way as a wave approaching from the left. This is not true of flow field refraction where the propagation velocity of a wave traveling in the same direction as a local flow field would be effected in a sense opposite to that of a wave propagating against the flow field. The wave propagation velocity in a flow field is shown by Savitsky to be:

$$C = \frac{1}{2} \left[C_0 + \sqrt{C_0^2 - 4V_w C_0 \cos \alpha} \right]$$

where:

C = wave propagation speed in a flow field

C_0 = wave propagation speed outside the flow field

V_w = magnitude of the flow at a specific point in the field

α = Angle between the flow, at the specific point, and the ray path

If the flow vector at every point in a flow field can be defined with reference to a fixed coordinate system, the effect of the flow field on local propagation velocity, C , and hence on the refractive properties of the flow field can be computed. The complete mathematical expressions describing

the effect of a flow field as a refractive medium are detailed by Savitsky, in his report, pp. 17-24, and need not be repeated here.

Savitsky models a refraction field as an explicit mathematical function of a fixed coordinate frame and uses a computer to calculate the path of a specific wave ray. This is repeated for enough rays to give a good representation of the overall refractive effect. Wave crest lines can be shown by drawing continuous lines which are everywhere perpendicular to adjacent rays.

Examination of the mathematical equations describing surface wave refraction reveals several interesting points:

1. Refraction, or change in ray direction, is a function of the propagation velocity gradient at a point, not the velocity magnitude.
2. Propagation velocity is a function of position and direction within the flow field.
3. Refraction is inversely related to wave period.
4. A flow field with a symmetrical, continuously decreasing velocity profile moving in the same direction as the waves refracts waves out of the flow field.

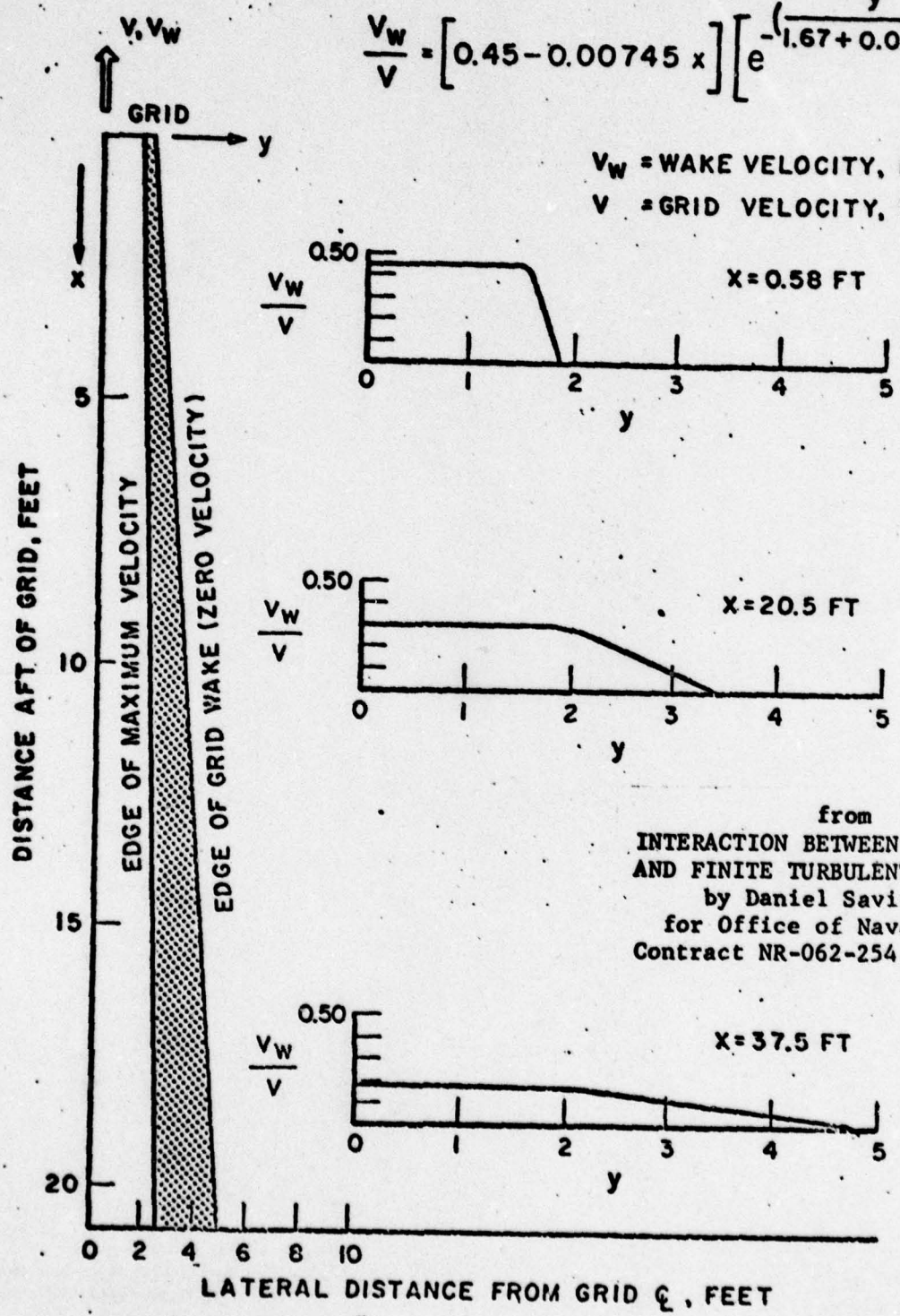
5. Diffraction and Superposition

Under some circumstances, a refraction diagram yields what are obviously erroneous results. For instance, in Savitsky's work, Fig. 3 shows a refraction diagram for the flow field generated by a towed grid. This flow field has a constant flow velocity over its central portion and so the flow velocity gradient and wave propagation gradient are zero for waves

GRID WIDTH = 36" , DRAFT = 20" , MESH SIZE = 2.7"
 (GRID TOWED IN 75 FT WIDE TANK)
 VELOCITY PROBE AT 10" DRAFT

$$\frac{V_W}{V} = [0.45 - 0.00745 x] \left[e^{-\left(\frac{y}{1.67 + 0.062 x}\right)^8} \right]$$

V_W = WAKE VELOCITY, FT/SEC
 V = GRID VELOCITY, FT/SEC



from
 INTERACTION BETWEEN GRAVITY WAVES
 AND FINITE TURBULENT FLOW FIELDS
 by Daniel Savitsky
 for Office of Naval Research
 Contract NR-062-254, Nonr263(36)

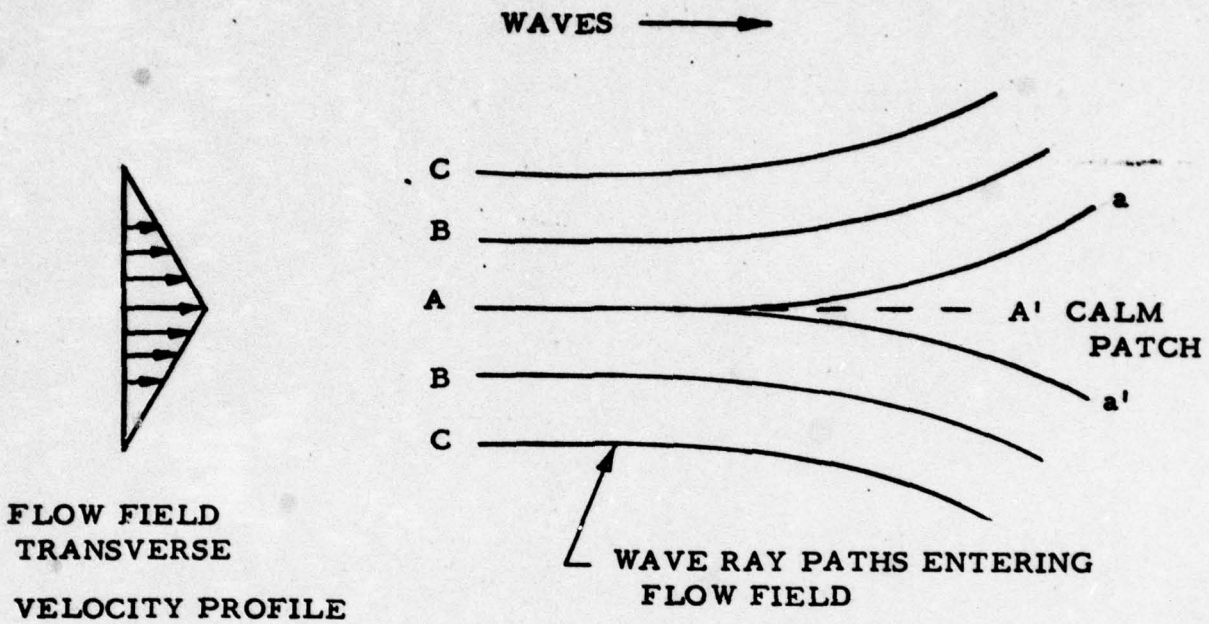
FIG. 3 LONGITUDINAL VELOCITY DISTRIBUTION IN GRID WAKE

with rays parallel to the flow field axis. This means that the waves in the central portion of the flow field would pass right through the flow field without being attenuated. Savitsky's experimental results indicated that this was not the case, and that the waves were reduced significantly more than predicted by pure refraction.

Another case which yields suspect results is the case of refraction by a sharply peaked flow field as shown in Fig. 4. This is similar to the acoustic shadow zone of Fig. 2, and analysis of this refraction diagram reveals that because the flow field gradient changes sign at its center, the ray, A, directed right at the center would be diverted along ray paths "a" and "a'." Since this ray is "split", a pure refraction diagram predicts a region of no waves or a "calm patch" analogous to an acoustic shadow zone which is intuitively suspect.

The solution to both these dilemmas is to consider wave diffraction along with refraction and use the theorem of superposition to find the effect when both occur at the same time.

Fig. 5 shows diffraction of a wave through a slit in a breakwater. This situation is analogous to this towed grate flow field in that the constant velocity portion of the flow field behaves as a slit while the flow gradients at each end act as "breakwaters" by refracting waves that pass through them. When this breakwater diffraction phenomenon is superimposed on the refraction diagram, the predicted wave amplitudes agree much more closely with those measured as shown in Savitsky's data Figs. 6, 7.



CALM PATCH PRODUCED BY A SHARPLY
PEAKED FLOW FIELD

FIGURE 4

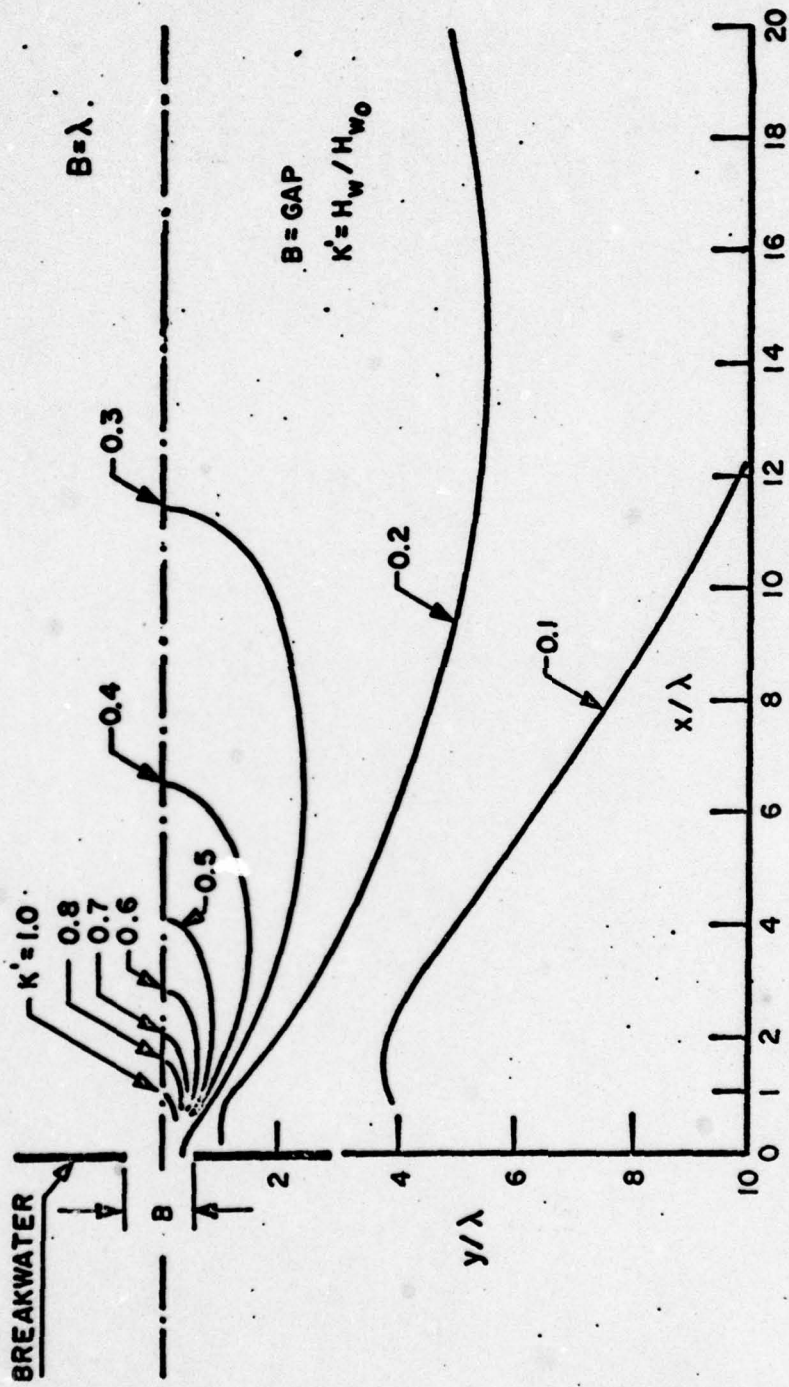


FIG. 5 DEFRACTION OF WAVES AT BREAKWATER GAP CONTOURS OF EQUAL DEFRACTION COEFFICIENT (JOHNSON 1952)

from
**INTERACTION BETWEEN GRAVITY WAVES
 AND FINITE TURBULENT FLOW FIELDS**
 by Daniel Savitsky
 for Office of Naval Research
 Contract NR-062-254, Nonr263(36)

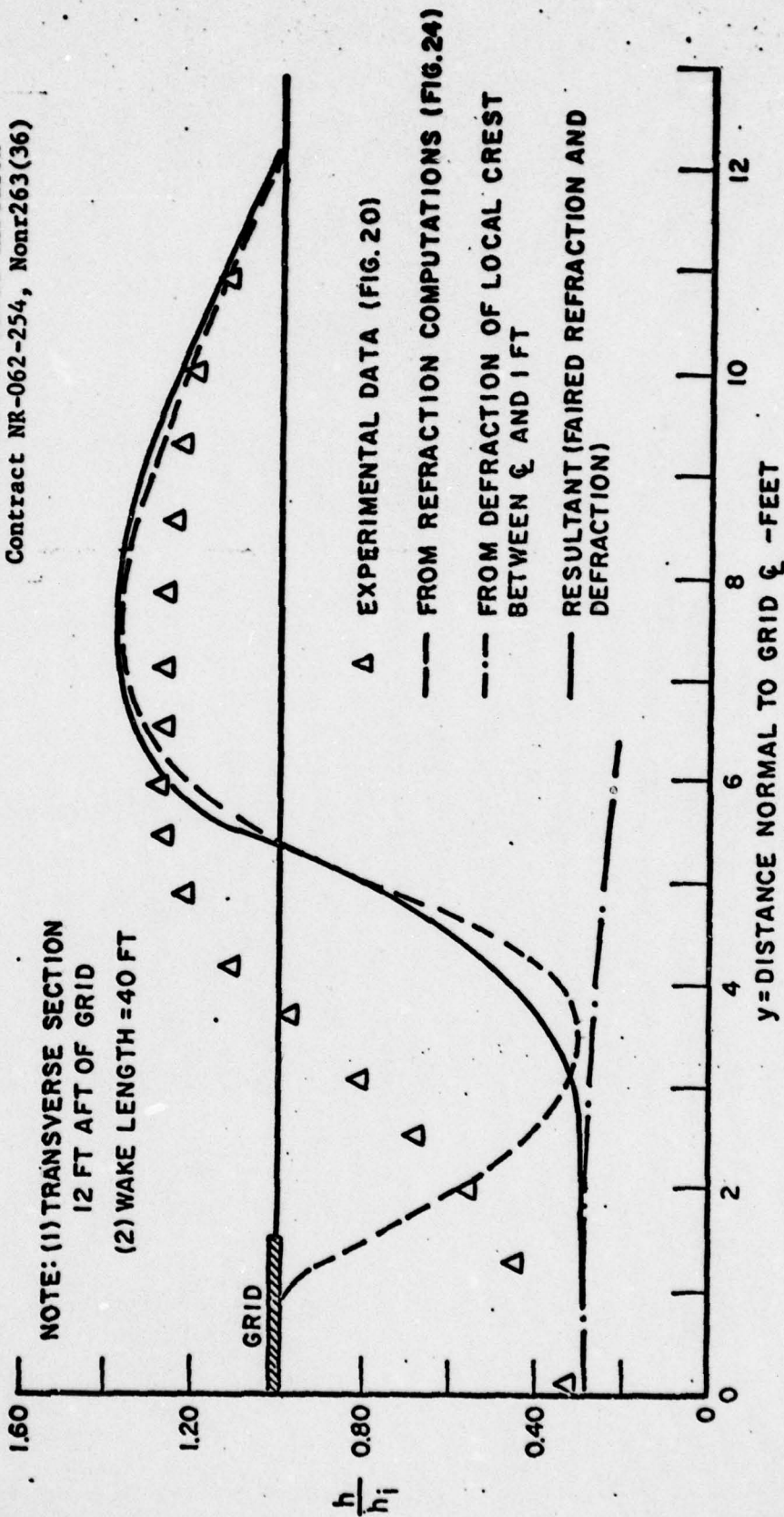


FIG. 6 COMPUTED VERSUS MEASURED CREST HEIGHT
 $\lambda = 6'$ $H_w = 1''$ GRID WIDTH = 3' MESH = 2.7" DRAFT = 1.67" $V = 1$ FT/SEC

from
**INTERACTION BETWEEN GRAVITY WAVES
 AND FINITE TURBULENT FLOW FIELDS**
 by Daniel Savitsky
 for Office of Naval Research
 Contract NR-062-254, Nonr263(36)

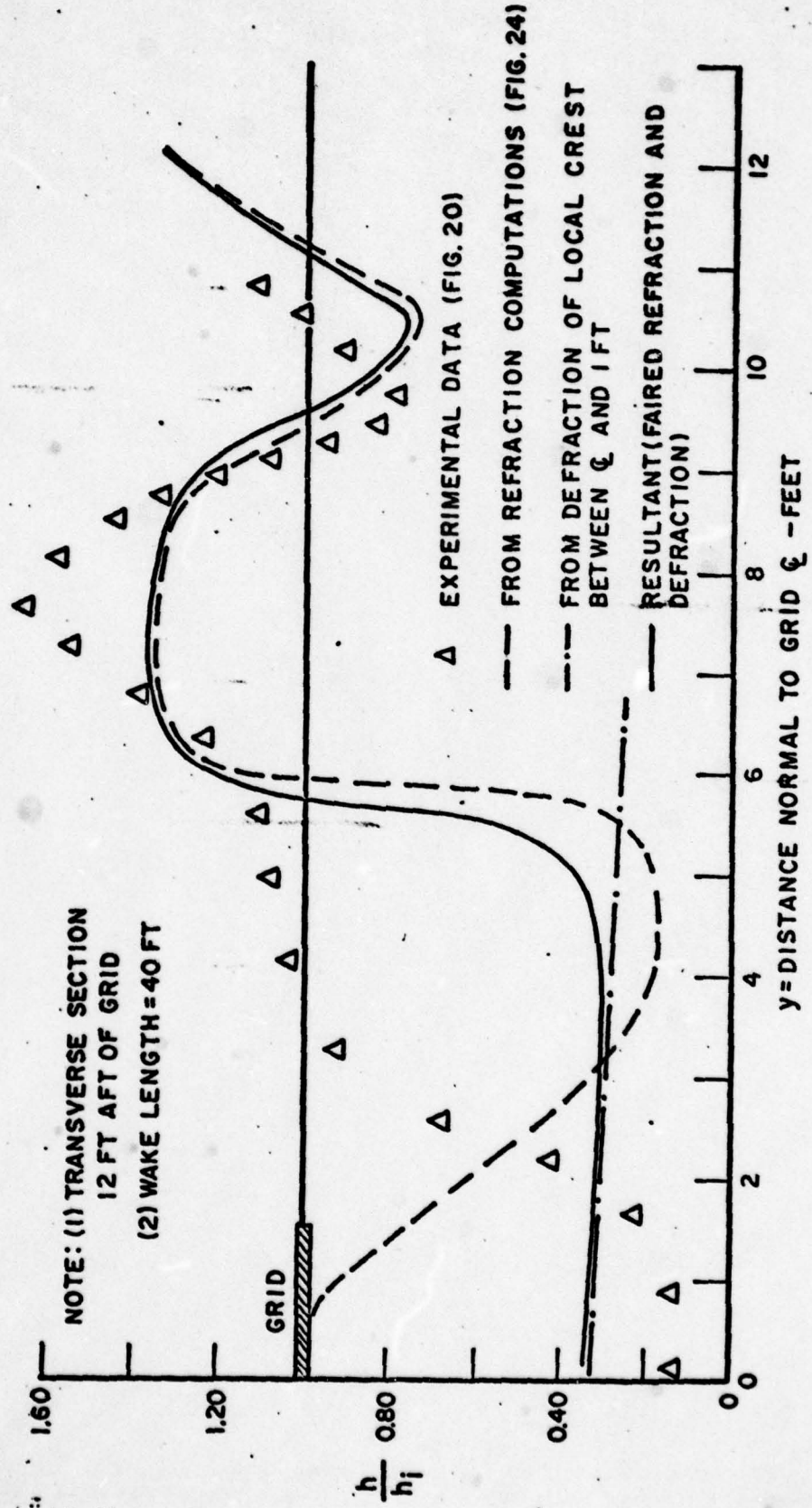


FIG. 7 COMPUTED VERSUS MEASURED CREST HEIGHT
 $\lambda = 2'$ $H_w = 1''$ GRID WIDTH = 3' MESH = 2.7" DRAFT = 1.67" $V = 1$ FT/SEC

The sharp peaked flow field of Fig. 4 also has a related diffraction phenomenon. Inspection of Fig. 4 shows that the rays all leave the flow field at about the same angle. The Line A-A' could be replaced by a breakwater wall since every wave above A-A' has a mirror image below A-A'. Diffraction of waves along a breakwater wall at an angle to wave ray paths has been analyzed, and the results can be applied to the sharp peaked velocity profile.

6. Ocean Wave Directional Spectrum

In order to apply the preceding analysis to the case of a fully developed, wind driven sea, the apparent difference between the regular train of waves modeled in refraction diagrams and the irregular waves of the open ocean must be accounted for. This difference can be explained by showing that the surface of the ocean can be described mathematically by assuming that waves in a particular region are the sum of a spectrum of waves of various lengths and amplitudes coming from various directions. This kind of analysis has been carried out and one of the most complete analysis of a wind driven wave directional spectrum was done by Cote et al (1960), and is referred to as the Stereo Wave Observation Project, SWOP. Their work has resulted in a contour plot (Fig. 8) which gives wave length and relative wave energy as a function of direction for sea state 4. Quantitative results of their analysis will be used later.

7. Oceanographic Research Ship

The ship selected for analysis was the AGOR-4 type. Stevens Institute of Technology carried out a dynamic analysis of this ship for its response

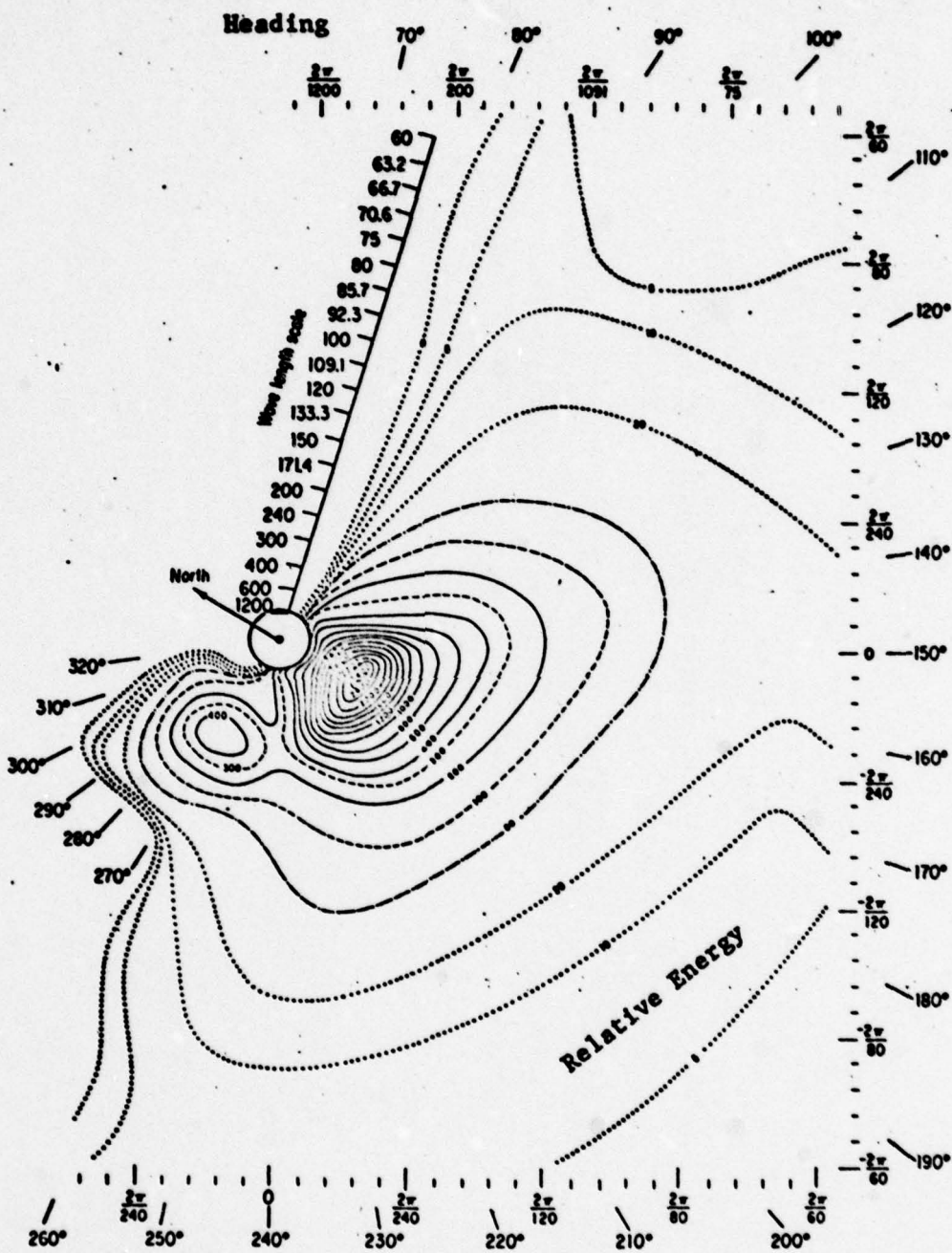


Fig. 8 Final Directional Wave Energy Spectrum from SWOP. Cote et al. (1960)

to waves over a range of wave periods in sea states 3 and 4. This analysis is included in Appendix A. This analysis shows that this vessel has its greatest response in both heave and pitch to waves of about 200 to 250 feet wave length which correspond to periods of about 6 - 7 seconds.

8. Calculations

All calculations will utilize the refractive flow field generated by Savitsky with the following parameters:

Grid Width = 3 ft.

Depth = 0.84 ft.

Mesh = 2.7 in.

Grid Tow Speed = 1 ft/sec.

Drag = 1.5 lbs.

Wave length = 6 ft.

The calculations are not intended to represent design parameters. They are, however, the best means available for modeling a refractive flow field of a size sufficient to reduce ship motions in a fully developed sea. Froude number scaling by wavelength is used for wave phenomenon while Reynolds number scaling by wave length is used for flow phenomenon.

9. Energy Required to Generate a Refractive Flow Field

In order to get a feel for the power required to generate a refractive flow field Savitsky's experimental results can be scaled as follows: where the subscript, S, refers to data measured by Savitsky and the subscript, P, refers to an open ocean prototype.

$$P = F V$$

P = Power

F = Drag Force

V = Velocity

The scaling factor used is the wavelength where:

$$\lambda_s = 6 \text{ FT.} \quad \lambda_p = 250 \text{ FT.}$$

λ_p is the maximum wavelength which would interfere most with ship operations over the stern or side as determined from the AGOR-4 ship motion study.

$$P = D V$$
$$P \quad P \quad p$$

Power = Drag Force x Velocity

For dynamically similar flow the drag coefficients for the test and prototype grids will be the same:

$$C_{DP} = C_{DS} = \frac{D_p}{(\rho_p V_p^2/2) A_p} = \frac{D_s}{(\rho_s V_s^2/2) A_s}$$

where the fluid densities ρ_s and ρ_p are equal. The areas, A, are related by:

$$\frac{A_p}{A_s} = \frac{L_p^2}{L_s^2}$$

Froude scaling is used for the velocities since the ratio of the wave propagation velocity to the flow field velocities must be identical for a similar refractive effect, and:

$$\frac{V_p}{V_s} = \left(\frac{L_p}{L_s} \right)^{\frac{1}{2}}$$

Combining all of the above equations the horsepower required is:

$$P_p = D_s V_s \left(\frac{L_p}{L_s} \right)^{\frac{7}{2}} = \frac{(1.5 \text{ LB}) (1 \text{ FT./SEC.}) \left(\frac{250 \text{ FT.}}{6 \text{ FT.}} \right)^{\frac{7}{2}}}{550 \text{ FT.-LB./SEC HP}}$$

$$P_p \doteq 1300 \text{ HORSEPOWER}$$

The working area of attenuated wave activity generated under the above conditions would be about 125 feet wide. A narrower working area would, of course, require less power.

10. Expected Attenuation in a Fully Developed Wind Driven Sea

Wave energy within the flow field will get there by two paths. They are:

1. Energy contributed by waves which approach at an angle too great to be refracted, and
2. Energy contributed by diffraction of refracted waves.

In order to estimate the effect of a refractive flow field in the directional spectra of a fully developed sea, the angle of approach throughout which refraction takes place must be determined. A computer program was written at OSE using a simplified set of refraction equations and run for a variety of wave approach angles with respect to the flow field axis. It was found that the maximum angle of effective refraction is approximately equal to the angle at which a ray, originally parallel to the flow field, leaves the flow field. In Fig. 9, this is angle α , and is about 25 degrees. This flow field will thus be effective throughout an included angle of 50°. It should be noted that a wider flow field of identical velocity gradient will effectively refract throughout a greater included angle.

From the directional spectra, Fig. 8, the percent of the 250 foot

from
**INTERACTION BETWEEN GRAVITY WAVES
 AND FINITE TURBULENT FLOW FIELDS**
 by Daniel Savitsky
 for Office of Naval Research
 Contract NR-062-254, Nonr263(36)

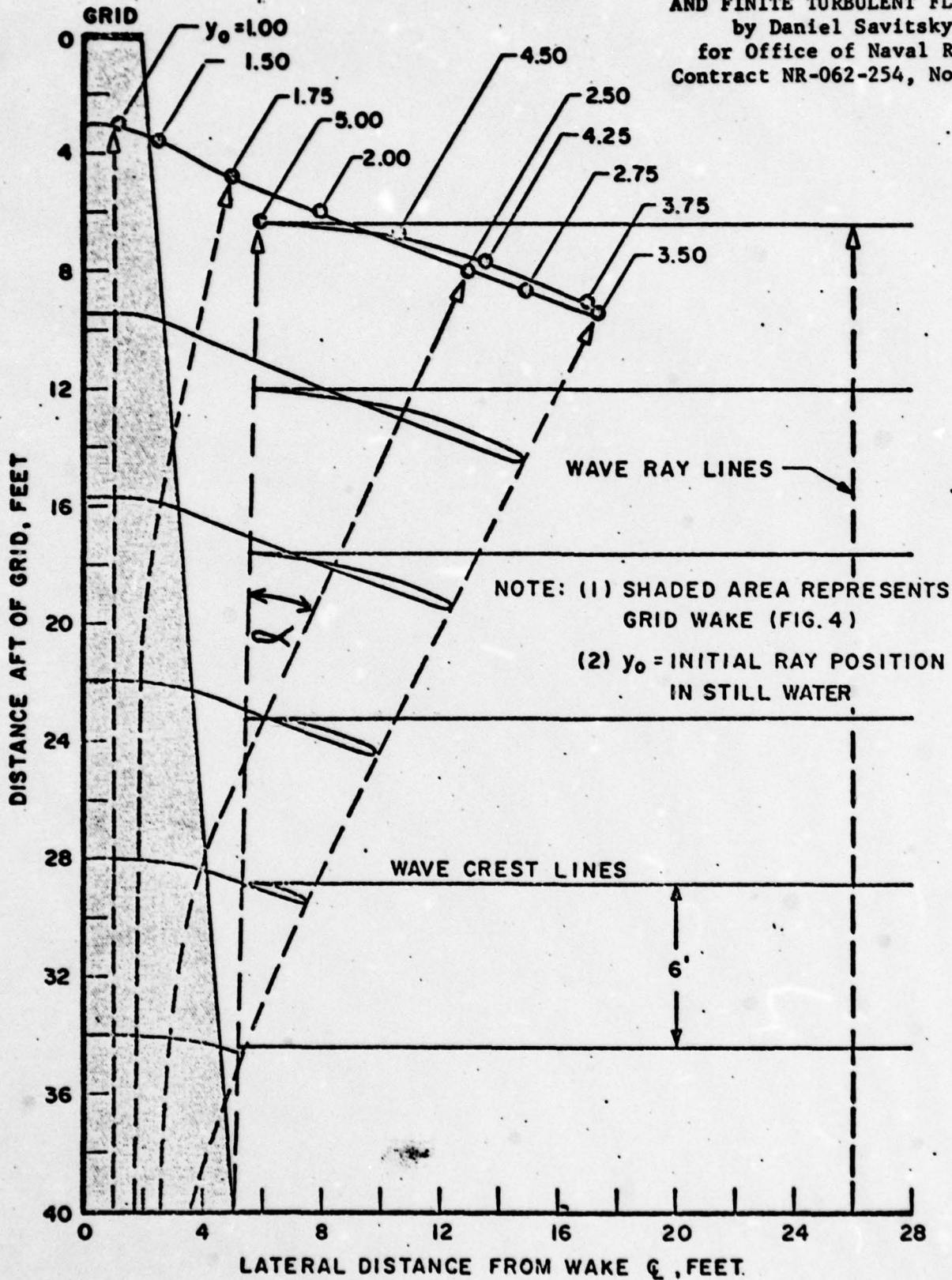


FIG. 9 COMPUTED WAVE REFRACTION DIAGRAM
 $\lambda = 6'$ $v = 1 \text{ FT/SEC}$

wavelength energy entering the refractive flow field at an angle ($\pm 25^\circ$) shallow enough to be completely refracted is 58%, or conversely, 42% of all available 250 foot wavelength wave energy gets into the refractive flow field.

Diffraction of non-refracted wave energy also must be included, and from Savitsky's test data Fig. 10, the height attenuation is:

$$\frac{h_{\text{field}}}{h_{\text{initially}}} = 0.5 \quad \text{(Fairly representative of all 6 foot wavelength data)}$$

so the energy attenuation is

$$\frac{e_f}{e_i} = \left(\frac{h_f}{h_i}\right)^2 = 0.25$$

So, 25% of refracted wave energy must be added to the non-refracted wave energy to arrive at the total wave energy in the refractive flow field.

The net wave energy in the flow field for a 250 foot length wave relative to the open ocean energy is:

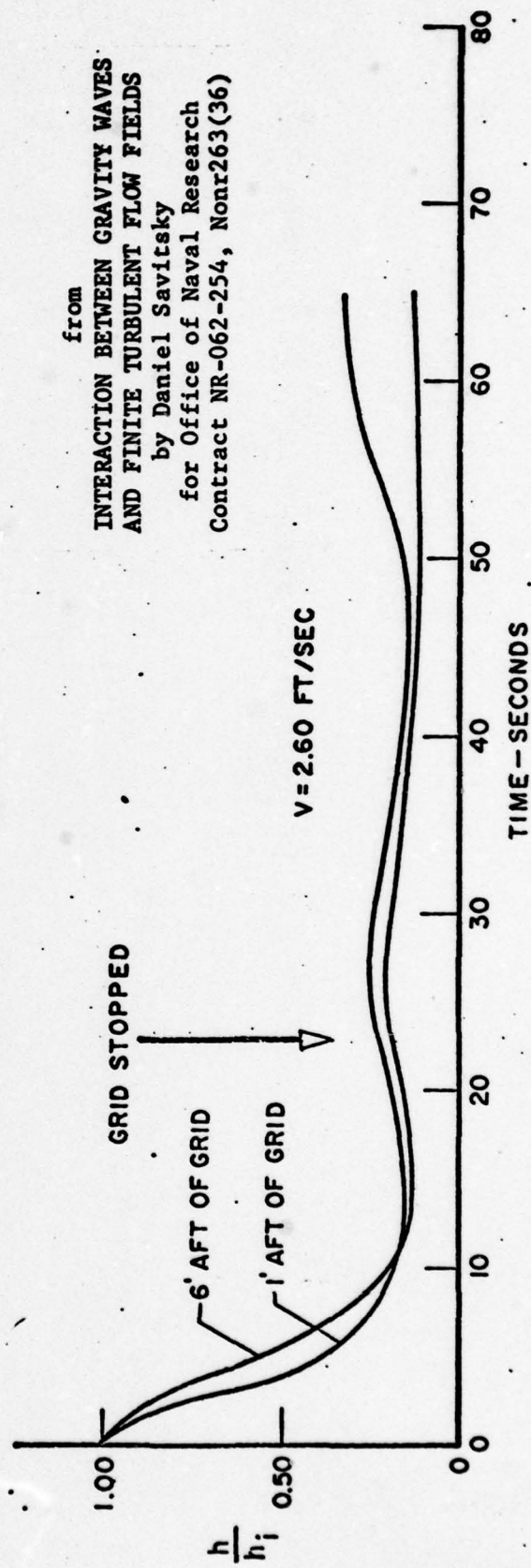
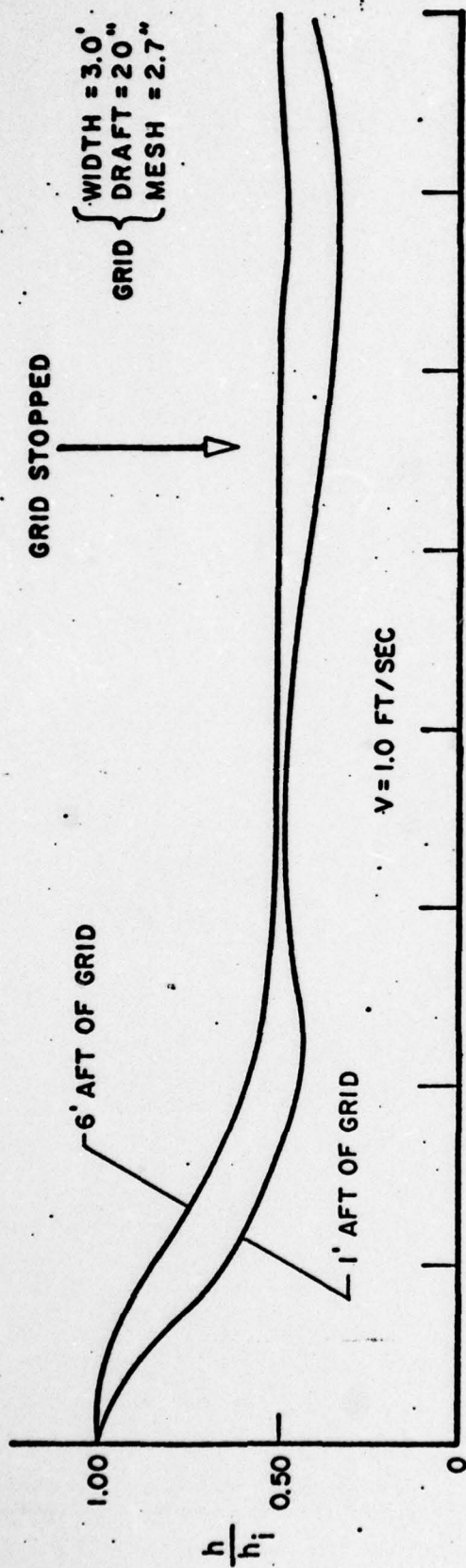
$$\frac{E}{E_i} = \text{Non Refracted} + \text{Diffacted} = .42 + (.25).58$$

$$\frac{E}{E_i} = .565$$

Or about 56% of the total wave energy available in the 250 foot wavelength is transmitted into the refractive field. Thus, attenuation of all 250 foot open ocean wave energy will be 44%. Greater attenuation will occur for all wavelengths less than 250 feet.

11. Time Estimate of Refractive Effect Persistence

Time estimated can be made from Savitsky's data by use of Fig. 10 where attenuation is plotted as a function of time. Since this is a flow phenomenon involving inertia and fluid viscosity, Reynolds scaling is used



from
INTERACTION BETWEEN GRAVITY WAVES
AND FINITE TURBULENT FLOW FIELDS
by Daniel Savitsky
for Office of Naval Research
Contract NR-062-254, Nonr263(36)

FIG. 10 ENVELOPE OF WAVE HEIGHT AT WAVE PROBES MOVING IN WAKE OF 2-DIMENSIONAL GRID
 $\lambda = 6'$ $H_w = 1.0''$

and:
$$\frac{t_p}{t_s} = \left(\frac{L_p}{L_s} \right)^2$$

or, time is scaled as the length squared. Scaling by wavelength:

$$t_p = t_s \left(\frac{\lambda_p}{\lambda_s} \right)^2 = \frac{25 \text{ SEC.}}{3600 \text{ SEC/HR.}} \left(\frac{250 \text{ FT.}}{6 \text{ FT.}} \right)^2 = 1.2 \text{ HOURS}$$

The 25 seconds used as t_s is the time shown in Fig. 10 between stopping the grid and the end of the data record. Refractive wave height attenuation was nearly constant at 0.5 throughout this time period.

12. General Properties of Refractive Flow Fields

Before discussing methods of generating and using refractive flow fields, it is useful to generalize pertinent points.

- The wave refraction effect of a local flow field is an experimentally measured analytically defined phenomenon.
- Superposition of diffraction effects on refractive effects must be used to explain measured refraction anomalies.
- Flow field velocity gradient and width determine the dimensions of the attenuated area and the amount of attenuation.
- Shorter wavelengths are more effectively refracted, all wavelengths are affected.
- The refraction phenomenon completely diverts a portion of the wave energy rather than partially attenuating all of it.
- When applied to a fully developed wind driven sea, the directional energy spectra of the sea must be considered.

- About half of the wave energy entering the refractive field will be that which enters the field at angles too great to be effectively refracted.
- The wake of a ship is refractive due to the flow field generated by the propeller wash.
- Ships' wakes have been used in the past for launching and recovering operations.
- Froude and Reynolds scaling indicate the following parameters for 250 foot wave refraction in a fully developed sea:

Field Wave Energy	56%
Field Wave Height	75%
Field Width	125 feet
Horsepower Required	1300 HP
Field Life	1.2 hrs.

13. Application of Refractive Flow Field to Ocean Operations

Any flow field oriented in the same direction as wave travel will attenuate waves if the flow field velocity gradient decreases continuously from a maximum. The amount of attenuation, and time duration will depend on the size and shape of the field.

In consideration of the projected horsepower requirement, the most promising approach to generating a flow field would be to utilize the ship's main propulsion equipment. This could be done directly by using the ship's propeller wash to drive the flow field, or to use the ship to propel a "grid" and approximate Savitsky's test conditions. The projected flow field persistence suggests that a recovery or implant operation be divided into two sequential phases, generating a refractive flow field, and object handling.

Use of the ship's propeller wash is supported by observations that the wake of a ship headed into the seas is an area of noticeable attenuation and that ships' wakes have been used for seaplane landing and recovery. Evidence that the propeller wash maintains its continuity as a flow field is qualitatively supported by observation:

"There are rather definite experimental indications (Albertson, M. L., Dai, Y. B., Jensen, R. A., and Rouse, H., ASCE, 1950, Vol. 115, pp. 639-697) that a submerged liquid jet issuing into a large body of real liquid loses its identity rather rapidly by diffusion and the formation of unnumerable vortexes, say within an axial distance of about 5 jet diameters. On the other hand, there are equally definite indications that the under-water jet disturbance set up by a screw propeller is often detectable far astern, at distances of 50 or 100 disc diameters. Whether this is because of the rotation existing in a propeller-outflow jet, or because the jet-producing device is continually moving away from the jet already formed is not known. Nevertheless, the jet disturbance appears to maintain its identity or even to predominate in the midst of the potential, viscous, and wave wakes forming the overall body or hull wake." (Saunders, Hydrodynamics in Ship Design, 1957, Vol. I, p. 273)

A propeller wash flow field could be increased in size and effect by retarding the ship's forward motion while operating at maximum power. This would have the effect of imparting more energy and momentum to the water, per foot of forward travel. Reaction devices such as additional propellers or water jet propulsion units could be used, but they would need to be applied in such a way that the flow field generated by them would not interfere with the flow field of the main propulsion unit. For instance, if a ship with four right angle drives were to face two units forward and two aft, the units facing in the direction of wave travel would

generate a flow field causing the approaching waves to diverge, but the units facing in the opposite direction would create a field causing waves to converge in the vicinity of the ship.

A more encouraging approach would be to use flaps or a drogue to retard the ship (Figs. 11-14). The flaps shown in Figure 11 would tend to augment the propeller wash, while the drogues would need to be carried outside or beneath the flow field so as to not impede its development. These drogues could consist of fine meshed fish or shrimp nets which are easily handled with available equipment, and are in effect "grids constructed of small diameter cylinders" which exhibit high drag characteristics.

A net could also be used as a grid to generate a flow field similar to Savitsky's, Fig. 14. In this case, the ship would tow the net in the direction of wave advance. Some means of holding the net open would be required and the effect of the propeller wash on the flow field would have to be minimized since it is directed toward the advancing waves and would cause convergent refraction.

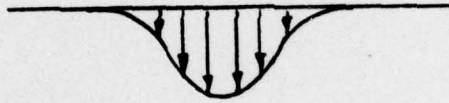
Any particular design application would require model tests duplicating the designed refractive flow field generation technique. Savitsky's tests were intended to investigate the effect of turbulence on waves and consequently cannot be expected to comprehensively define the refractive phenomenon.

In order to quantify the refractive effect of a flow field, a test

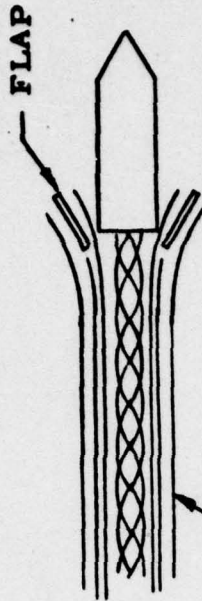
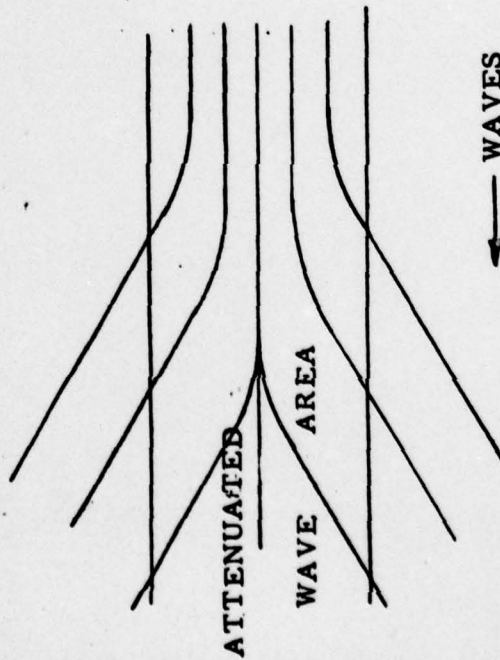


FLAP

VELOCITY
PROFILE



REFRACTIVE EFFECT

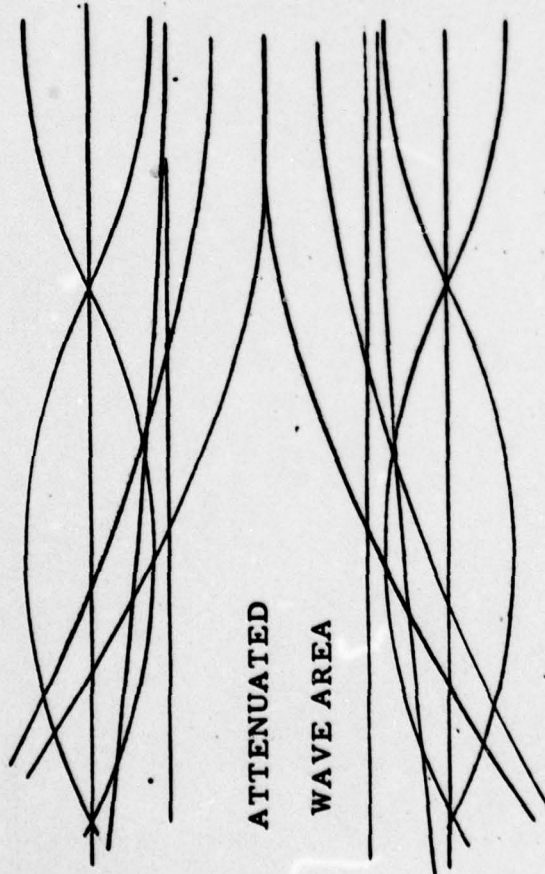


PROPELLER WASH
AUGMENTED BY FLOW
ALONG FLAPS

PROPELLER WASH UTILIZATION
WITH FLOW ALONG FLAPS

Figure 11

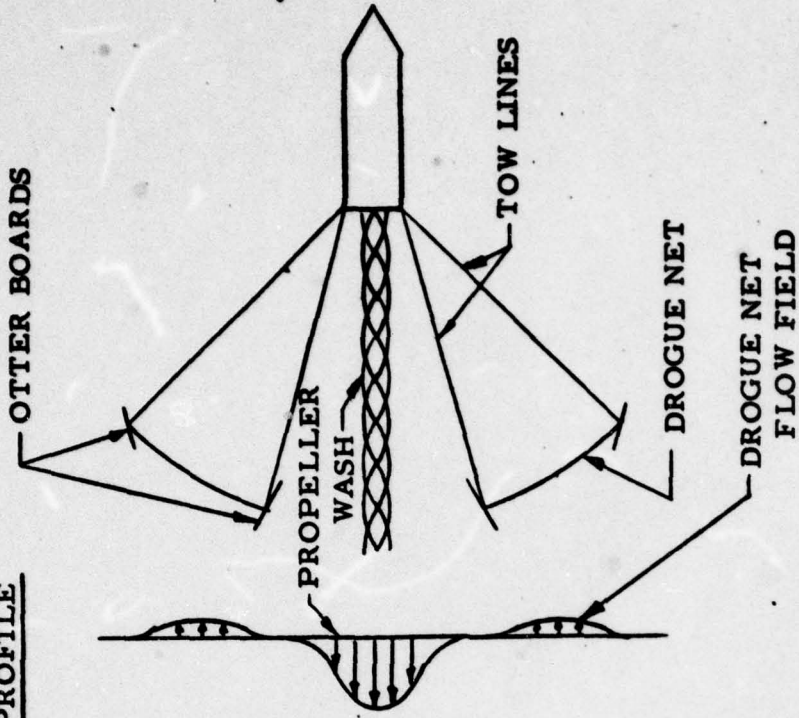
REFRACTIVE EFFECT



ATTENUATED
WAVE AREA

← WAVES

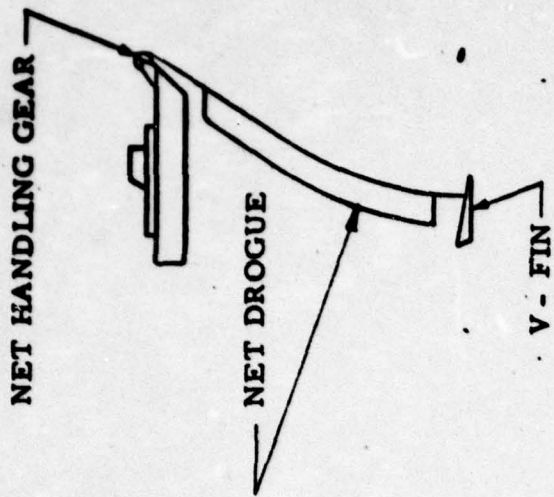
VELOCITY
PROFILE



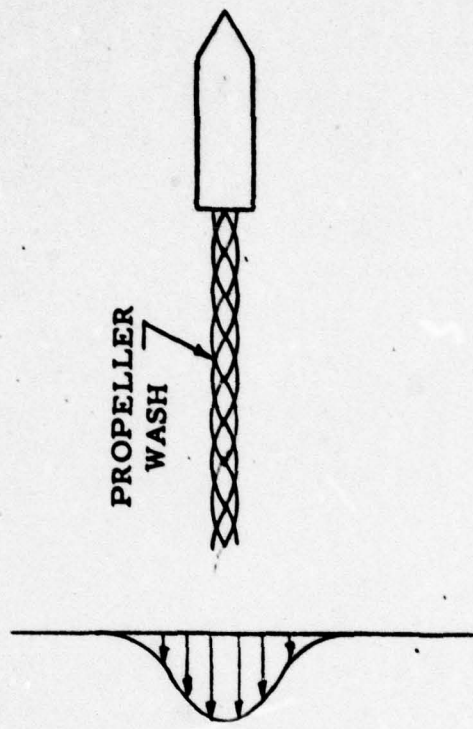
PROPELLER WASH UTILIZATION

WITH SIDE NET DROGUES

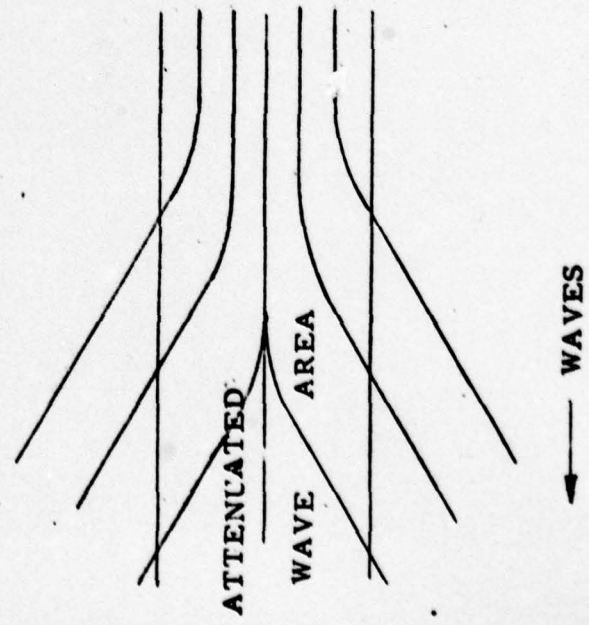
Figure 12



VELOCITY PROFILE

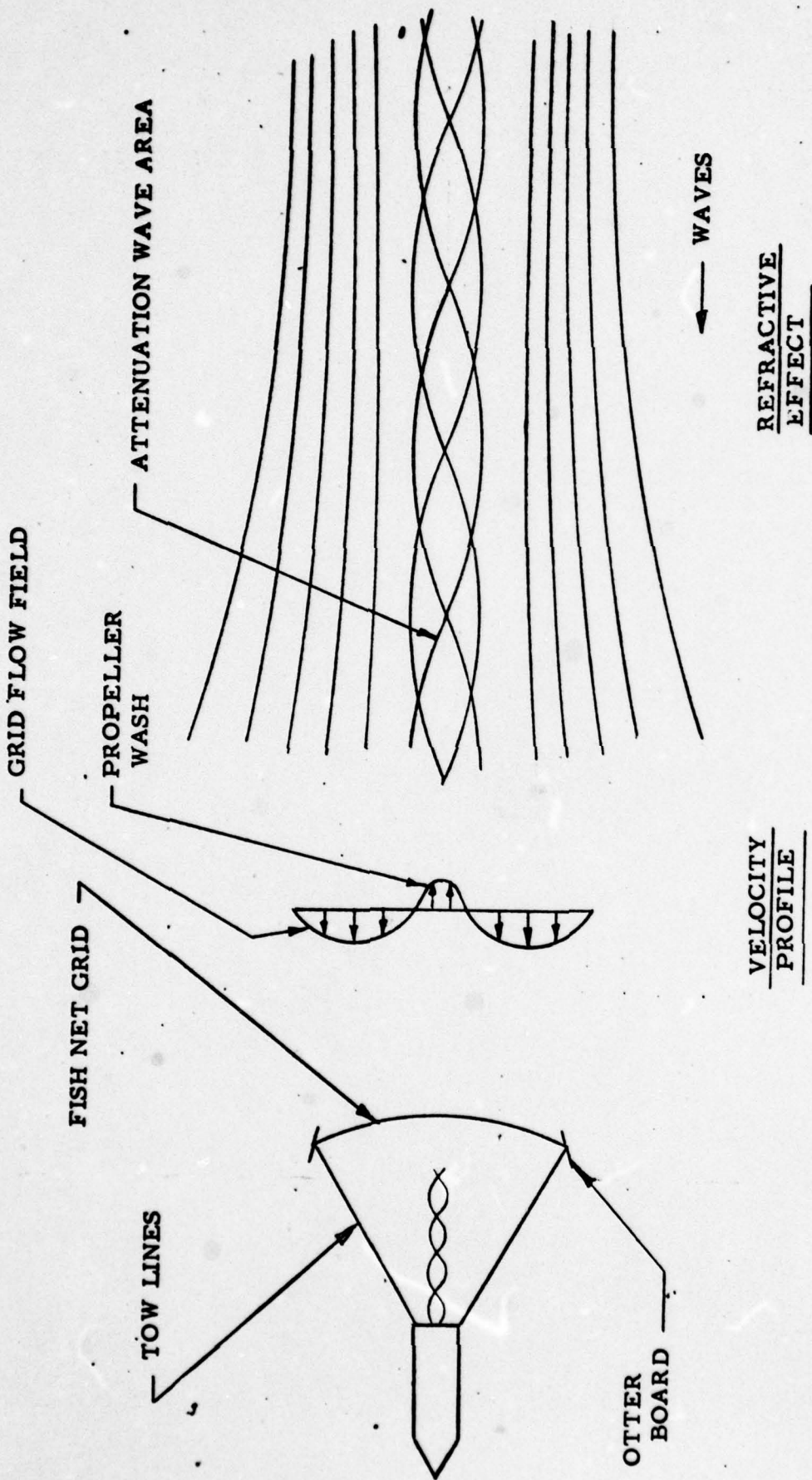


REFRACTIVE EFFECT



PROPELLER WASH UTILIZATION
WITH SUSPENDED NET DROGUE

Figure 13



FLOW FIELD GENERATED BY A TOWED GRID

Figure 14

series should be conducted to optimize the following parameters for maximum attenuation in a fully developed sea:

- Flow field velocity gradient
- Flow field width
- Flow field length
- Effective refraction persistence
- Power required

These tests should be designed with a particular generating technique in mind, such as using a ship's propeller wash, towing a grid, or other means. This test series would yield conclusive results concerning the practicality of using a ship generated refractive flow field for open ocean wave attenuation.

14. Recommendations

Recognizing that the ultimate goal of this study is to adapt a flow field generating device or technique to an AGOR-4 type vessel, it is recommended that intermediate testing be considered for Phase II of this study. It is more cost effective to do testing on a smaller scale to prove certain techniques before proceeding to a full scale system design. Therefore, it is recommended that a test series should be conducted using a small boat (100 ft.) in the open ocean to obtain basic data which would prove to a degree, the effectiveness of producing a flow field to attenuate waves in the open ocean. In addition, this series should include the investigation of propeller generated flow fields and flow fields generated by towing grids of various configurations. This test series should be based on the results obtained from Savitsky model tank investigations.

The test series should be designed to measure the generated flow field as a function of energy put into the water and the wave energy attenuation as a function of position in a flow field. This information will result in an engineering report and data which can be extrapolated to larger vessels such as the AGOR-4. With this engineering data, it can be readily determined if a flow field can be practically generated for a large vessel in the open ocean. If the investigation proves that this approach to open ocean wave attenuation is practically feasible, a flow field generating device or technique can be readily designed for adaptation to a larger vessel of the AGOR-4 type.

BIBLIOGRAPHY

- ARTHUR, R. S.
1950
Refraction of Shallow Water Waves: The Combined Effect of Currents and Underwater Topography. Transactions, American Geophysical Union, Vol. 31, Number 4, August, 1950. pp. 549-552.
- BARTBERGER, C. L.
1965
Lecture Notes on Underwater Acoustics. Alexandria, Virginia: Defense Documentation Center, pp. 80-122.
- BASCOM, W.
1964
Waves and Beaches. Garden City, New York: Doubleday and Company, Inc. pp. 69-77.
- COTE, L. J., J. O. DAVIS, W. MARKS, R. J. MCGOUGH,
E. MEHR, W. J. PIERSON, JR., J. F. ROPEK, G. STEPHENSON,
and R. C. VETTER
1960
The directional spectrum of a wind generated sea as determined from data obtained by the Stereo Wave Observation Project. Meteorol. Papers, N. Y. U., Coll. of Eng. 2(6)88 pp.
- KINSMAN, B.
1965
Wind Waves Their Generation and Propagation on the Ocean Surface: Englewood Cliffs, New Jersey: Prentice Hall, Inc.
- PUTNAM, J. A., ARTHUR, R. S.
1948
Diffraction of Water Waves by Breakwaters. Transactions, American Geophysical Union, Vol. 29, Number 4, August 1948. pp. 481-490.
- SAUNDERS, H. E.
1957
Hydrodynamics in Ship Design, Vol. I. New York, New York: The Society of Naval Architects and Marine Engineers. p. 273.
- SAVITSKY, D.
1970
Interaction Between Gravity Waves and Finite Turbulent Flow Fields. Stevens Institute of Technology. Report prepared for Office of Naval Research, Department of the Navy, under contract NR-062-254, Nonr 263 (36). 58 pp.

BIBLIOGRAPHY (continued)

STRAUB, L. G., BOWERS, C. E., TARAPORE, Z. S.
1959

Experimental Studies of Pneumatic and Hydraulic
Breakwaters. University of Minnesota. Technical
Paper No. 25, Series B. Minneapolis, Minnesota.
49 pp.

APPENDIX

**Motions of Oceanographic Research Ship
in Irregular Head Seas**

by

**Daniel Savitsky, Consultant
March 14, 1970**

MOTIONS OF OCEANOGRAPHIC RESEARCH SHIP IN IRREGULAR HEAD SEAS

by

Daniel Savitsky, Consultant
March 14, 1970
revised

OBJECTIVE AND BACKGROUND

In accordance with Ocean Science and Engineering, Inc. Purchase Order B 2009, dated 2-25-70, an analytical ship motion study was carried out to determine the wave frequencies most likely to result in the largest relative motions between the hull of a typical oceanographic vessel and launched/recovered objects which are essentially surface followers.

The surface ship selected for this study was an AGOR-4 type whose dimensions were specified within the enclosures contained in Ocean Science and Engineering, Inc. letter BPP/rm, dated 12 February 1970. For the purpose of this study, it was assumed that the craft was heading into irregular sea states 3 and 4 and was at zero speed. Further, it was desired to compute the relative motions between the ship and the local wave surface at the stern and at the C.G. in addition to the ship heave and pitch motion about the center of gravity. These calculations were required as Subtask A of ONR Contract No. N-00014-69-C-0256.

COMPUTATIONAL PROCEDURE AND RESULTS

The ship motion calculations for regular head seas were carried out using the computer program procedure described in Ref 1. Assuming the ship-wave system to be linear, the spectrum of ship motions in irregular head seas of state 3 and 4 were computed using the superposition concept as described in Ref 2. The following results are presented in this report.

1. Table I presents the particulars of the oceanographic ship considered in this study.
2. Table II presents a tabulation of the ship response per unit wave amplitude as a function of wave length in regular waves.

- Included in this tabulation are: the motion of the C.G. (z_a) and phase angle; the pitch angle (θ_a) about the center of gravity and phase angle; the motion of the stern relative to the local wave surface (h_a) and phase angle. Figure 1 describes the nomenclature for motions and phase angles used in this report.
3. Table III presents the response amplitude operators for z_a , h_a , and θ_a , required for evaluation of ship motion in irregular seas.
 4. Table IV presents the response amplitude operator for h_{CG} , (the relative motion between hull and local wave surface at ship center of gravity). These data are also plotted in Fig 5.
 5. Figure 2 presents plots of the response amplitude operators tabulated in Table III.
 6. Figure 3 presents plots of the wave energy spectrum for sea states 3 and 4. These spectra, correspond to the Pierson-Moskowitz formulation for deep water, fully developed seas (Ref 3). Included on these plots are the average wave height (H_T) and wave amplitude ζ_a , and the significant (1/3 highest) values of H_T and ζ_a .
 7. Figure 4 presents the motion response spectra for heave of center of gravity; pitch about center of gravity; and relative motion between stern and local wave surface at stern. Also included on Figure 4 are the statistical descriptions of motion including the average values and significant values (1/3 highest).
 8. Figure 6 presents the motion response spectra for the relative motion between hull and local wave surface at the ship center of gravity.

DISCUSSION

From Figures 4 and 6 it can be seen that the relative motion between hull and local wave surface are largest for a sea state 4 and are most pronounced for wave frequencies between .7 and 1.4 radians per second.

This corresponds to wave lengths between 400 ft and 100 ft. Further, excluding roll motions, the relative motions between hull and local wave surface are smaller at the C.G. position than at the stern position. It is also seen that the stern and C.G. motions relative to the local wave surface are particularly large at a wave frequency of approximately 1.1 radians per second which corresponds to a wave length of 170 ft.

The relative stern motions in sea state 3 are approximately 80% less than those in sea state 4 but nevertheless exhibit essentially the same troublesome wave lengths.

The absolute vertical motions at the center of gravity and absolute pitch motions about the center of gravity (Fig 4) are very small for both sea states.

REFERENCES

1. Jacobs, W.R., Dalzell, J. and Lalangas P. "Guide to Computational Procedures for Ship Motions." Davidson Laboratory, Stevens Institute Report 791, Oct. 1960.
2. St. Denis, M. and Pierson, W.J., Jr., "On the Motions of Ships in Confused Seas," Transactions SNAME 1955.
3. Moskowitz, L.; Pierson, W.J., Jr.; Mehr, E., "Wave Spectra Estimated From Wave Records," NYU, College of Eng. Research Div., 1962, 1963.

David S. ...
April 2, 1970

TABLE I

PARTICULARS OF OCEANOGRAPHIC RESEARCH SHIP
 (Obtained from BuShip Drawing No. AGS 25-800-2068178A)

LOA = 208'-4"

LBP = 196'-0"

Displacement, Total, = 1,350 tons

Pitch Radius of Gyration = LOA/4

LCG = 1.9' aft of Station 5

SECTION PROPERTIES

<u>Station</u>	<u>Beam</u>	<u>Draft</u>	<u>Section Area</u>	<u>Sect. Area Coeff.</u>
0.5	4.104 ft	12.750 ft	32.777 ft ²	.626
1	8.790	13.854	71.959	.591
2	19.582	13.948	175.306	.642
3	29.458	14.052	292.214	.706
4	36.125	14.146	388.352	.760
5	39.000	14.250	434.061	.781
6	39.082	14.344	410.637	.733
7	36.688	14.448	326.863	.617
8	31.440	14.552	209.199	.457
9	20.334	14.646	84.429	.283
9.5	11.668	3.320	19.400	.500

TABLE II

SHIP RESPONSE PER UNIT WAVE AMPLITUDE
TO REGULAR WAVES (HEAD SEA DIRECTION)
FOR ZERO SHIP SPEED

Wave Length	ω	C.G. Heave		C.G. Pitch		Relative Stern Motion	
		$\frac{z_a}{\zeta_a}$	ϵ^*	$\frac{\theta_a}{\zeta_a}$	ϵ^*	$\frac{h_a}{\zeta_a}$	ϵ^*
100 ft	1.42 rad/sec	.179 ft	-24.15°	.26°	-93.3°	1.05 ft	62.5°
150	1.16	.139	24.90	.63	34.0	1.35	-144.7
200	1.01	.313	81.27	1.00	20.8	1.37	-169.2
250	.90	.504	89.23	1.14	14.6	1.15	177.9
300	.82	.637	90.9	.98	11.1	.90	168.9
500	.64	.864	91.1	.69	5.5	.39	147.2
800	.50	.948	90.6	.45	3.0	.19	129.9

* Phase Angle (SEE FIG 1)

TABLE III

SHIP RESPONSE AMPLITUDE OPERATORS

Wave Length	ω	Heave $(\frac{z_a}{\zeta_a})^2$	Pitch $(\frac{\theta_a}{\zeta_a})^2$	Relative Stern Motion $(\frac{h_a}{\zeta_a})^2$
100 ft	1.42	.03	.07 deg ² /ft ²	1.10
150	1.16	.02	.40	1.85
200	1.01	.10	1.00	1.87
250	.90	.25	1.30	1.32
300	.82	.41	.96	.81
500	.64	.75	.47	.153
800	.50	.90	.20	.036

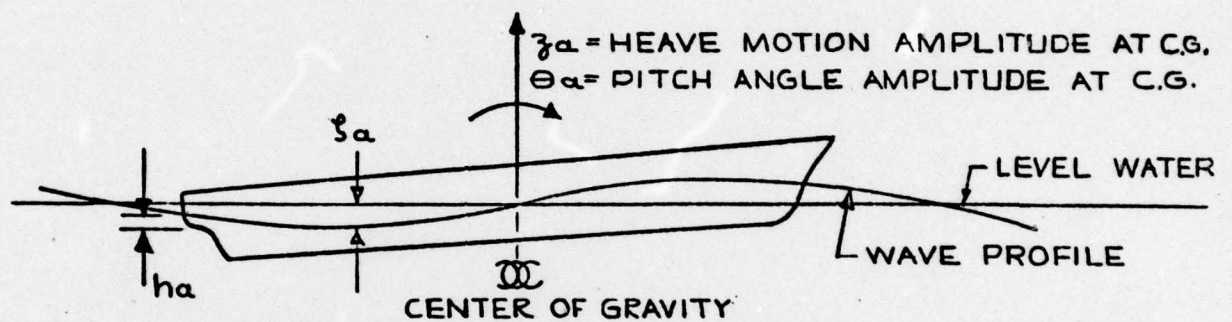
TABLE IV

RESPONSE AMPLITUDE OPERATOR FOR CENTER OF GRAVITY
MOTION RELATIVE TO LOCAL WAVE SURFACE :

λ	ω	$(h_{CG}/\zeta_a)^2$
100 ft.	1.42 rad/sec.	.90
150	1.16	.66
200	1.01	.46
250	.90	.25
300	.82	.13
500	.64	.02
800	.50	0

COORDINATE SYSTEM AND NOTATION TO ORIENT AXES OF SHIP
IN WAVES

← C_w = WAVE CELERITY
→ v = SHIP SPEED=0



h_a = HEAVE MOTION
OF STERN RELATIVE
TO WAVE SURFACE

h_{cg} = HEAVE MOTION AT C.G.
RELATIVE TO LOCAL
WAVE SURFACE

ADDITIONAL NOTATION

C_w = WAVE CELERITY $2.27 \lambda^{1/2}$, FT/SEC
 z_a = WAVE AMPLITUDE, FT
 λ = WAVE LENGTH, FT
 T = WAVE PERIOD, SEC
 ω = FREQUENCY $2\pi/T$, RADIANS/SEC
 ϵ = PHASE ANGLE BETWEEN C.G. AND
WAVE NODAL POINT, DEG.
 $\epsilon=0^\circ$ AS SHOWN IN SKETCH
 $\epsilon=90^\circ$ FOR WAVE CREST AT C.G.
 $\epsilon=270^\circ$ FOR WAVE THROUGH AT C.G.

FIGURE 1

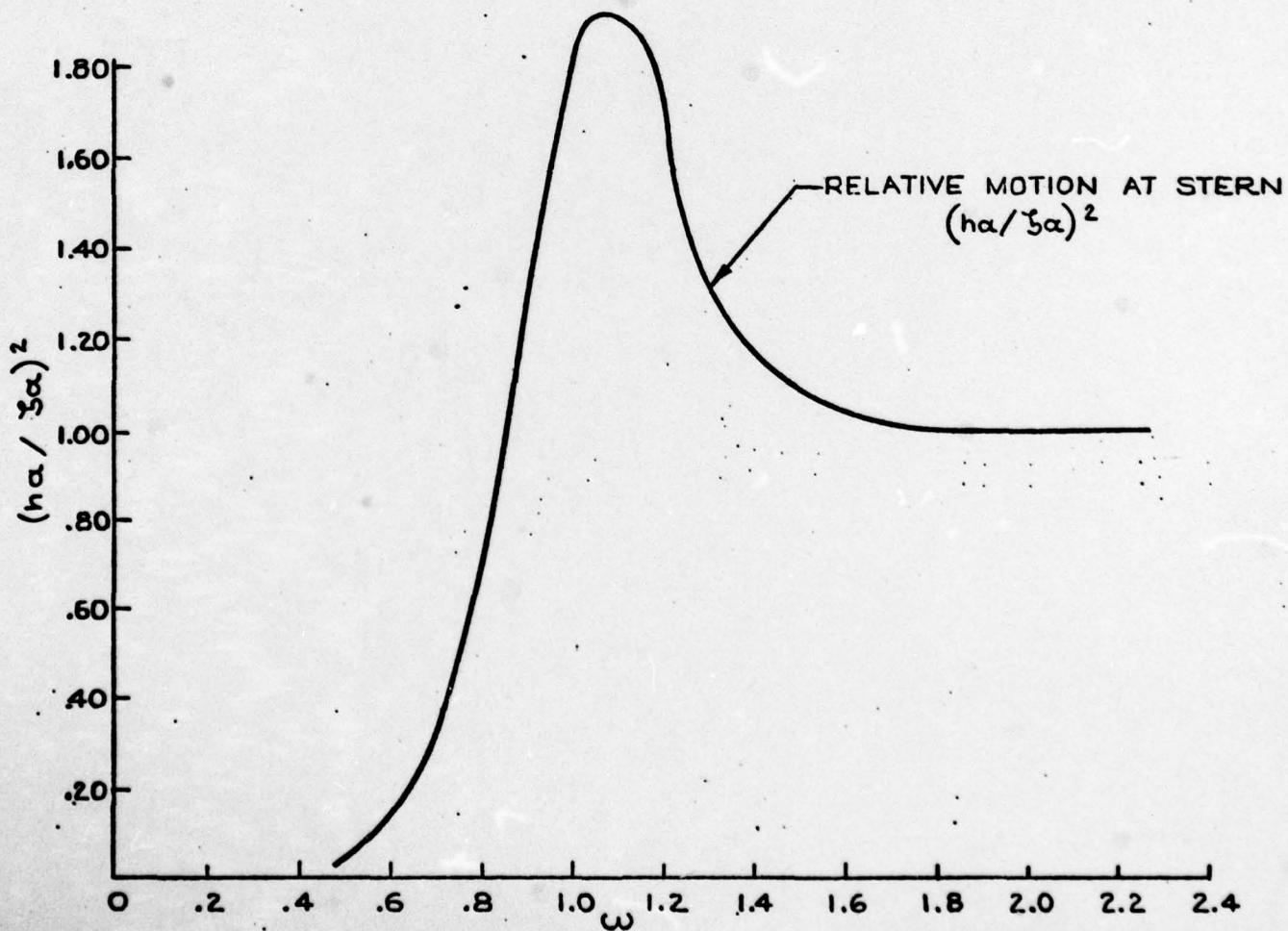
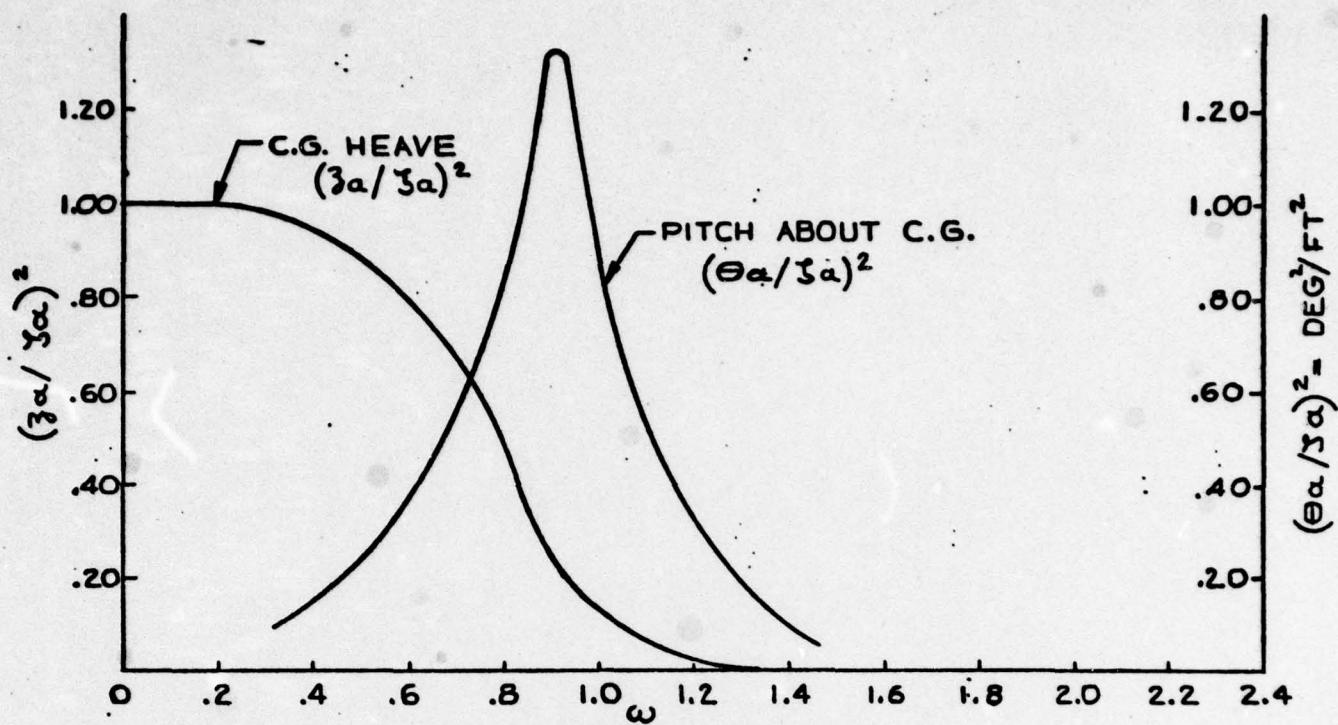


FIGURE 2
 RESPONSE AMPLITUDE OPERATORS

FIGURE = 3

WAVE ENERGY SPECTRUM IN IRREGULAR SEA
(PIERSON-MOSKOWITZ, FULLY DEVELOPED)

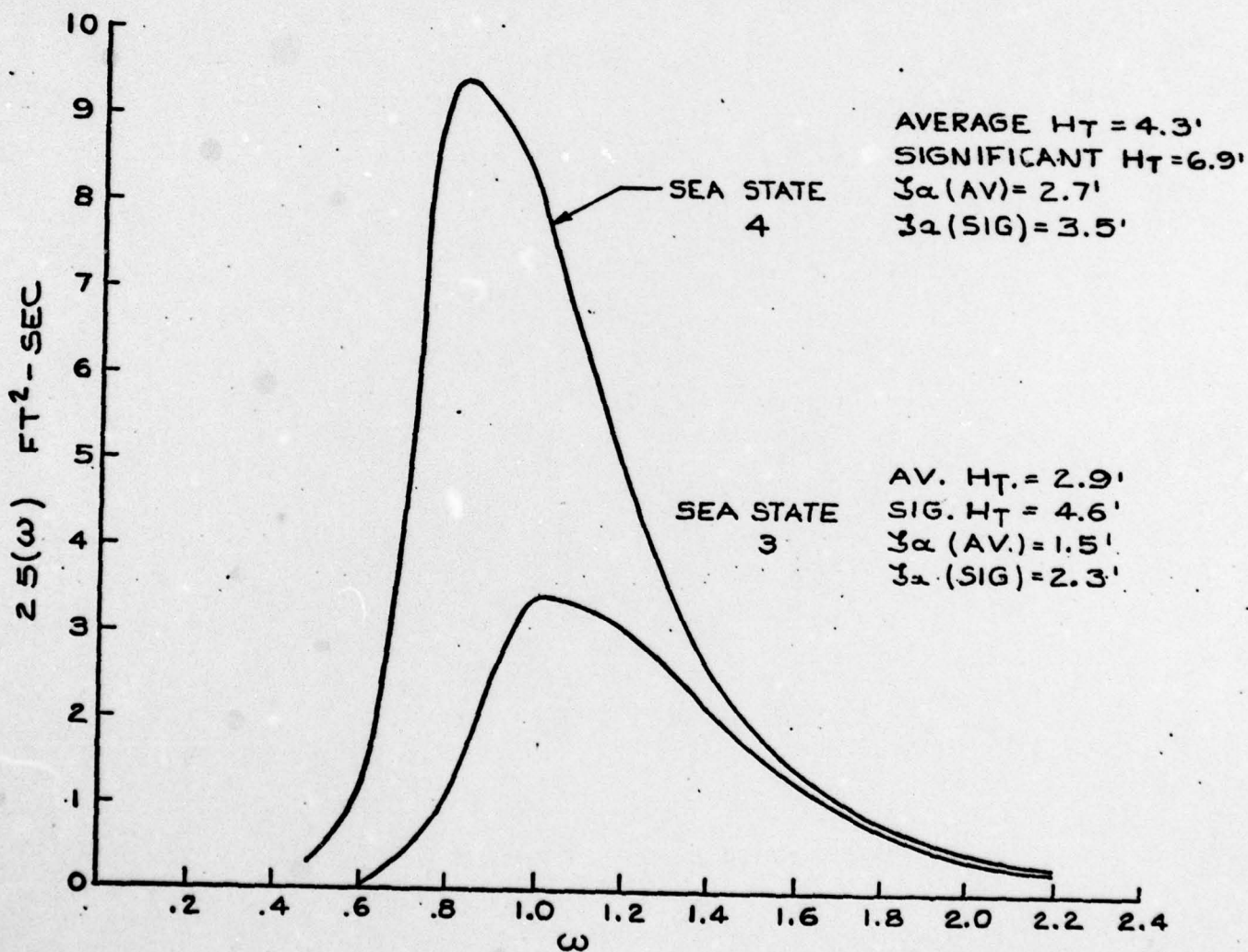


FIGURE 4

MOTION RESPONSE SPECTRA

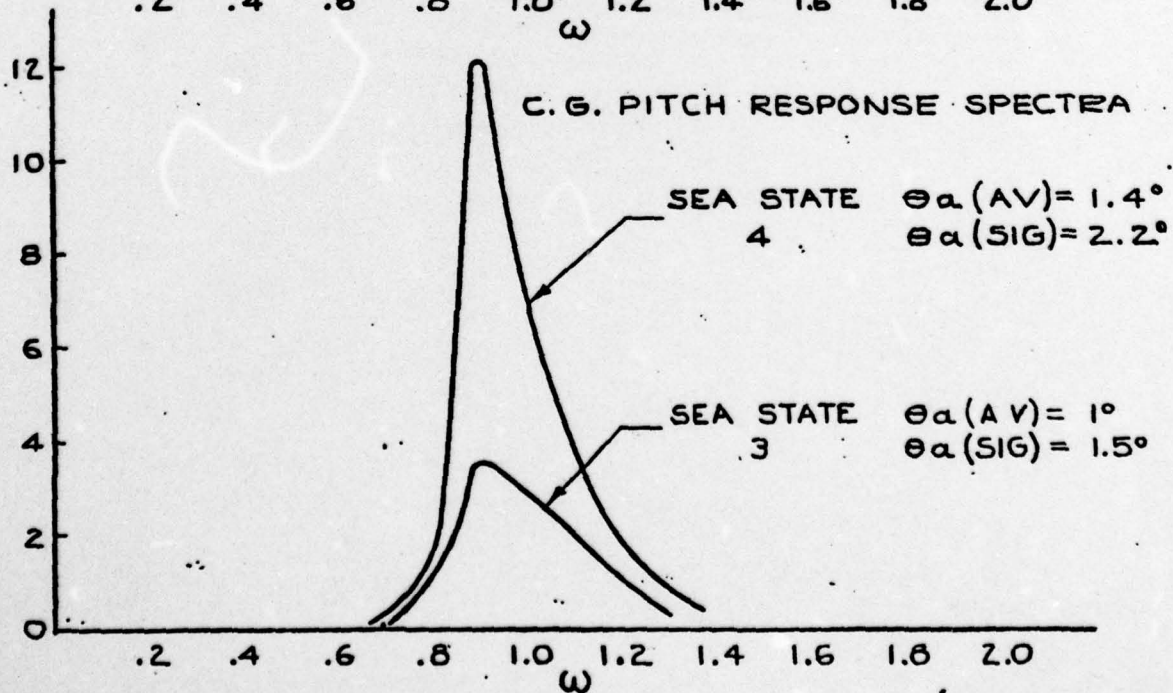
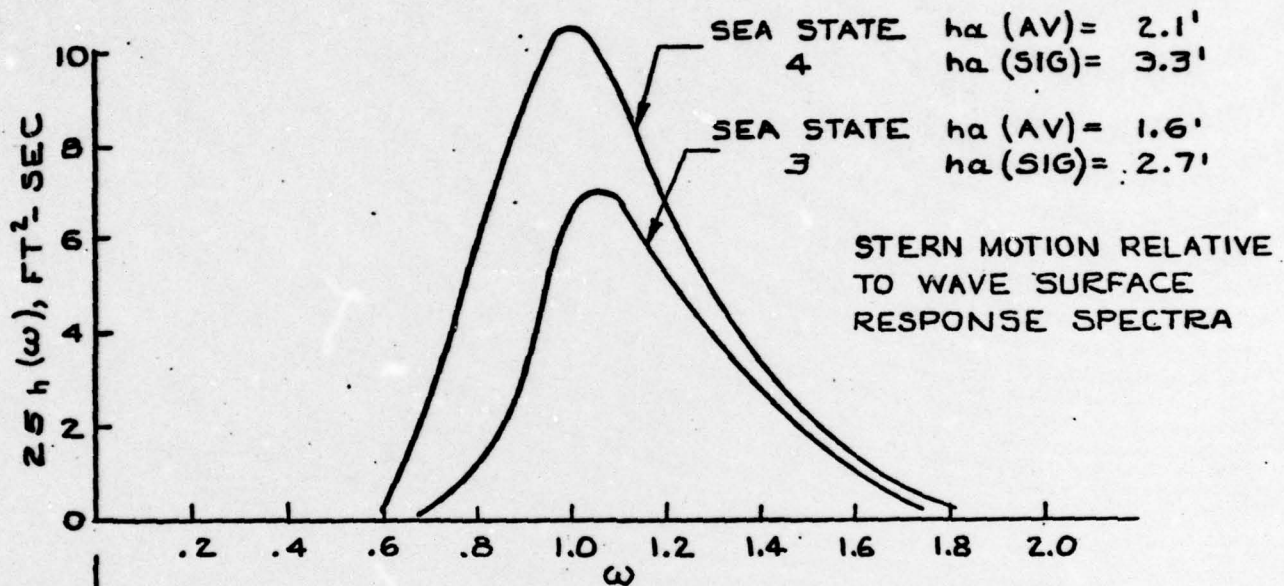
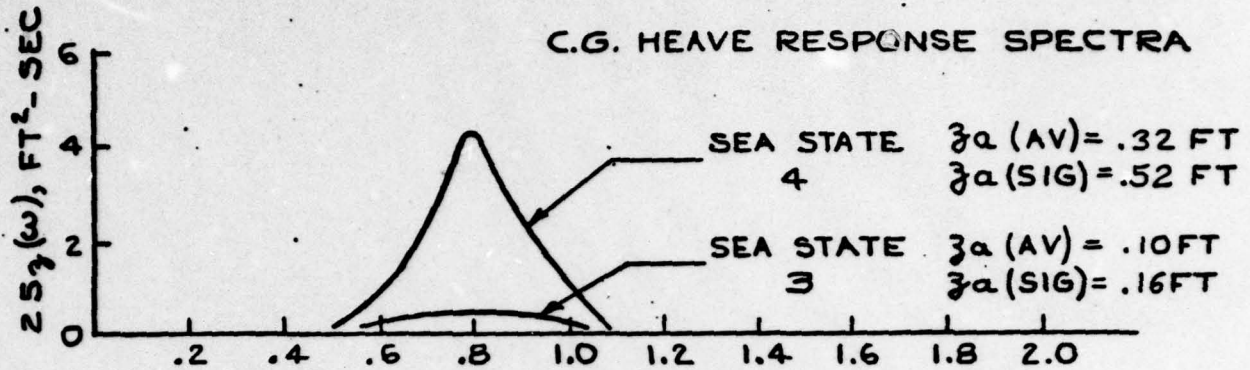


FIGURE 5
 RESPONSE AMPLITUDE OPERATOR
 RELATIVE MOTION BETWEEN SHIP AND LOCAL WAVE SURFACE
 AT CENTER OF GRAVITY
 $(h_{CG}/\zeta a)^2$

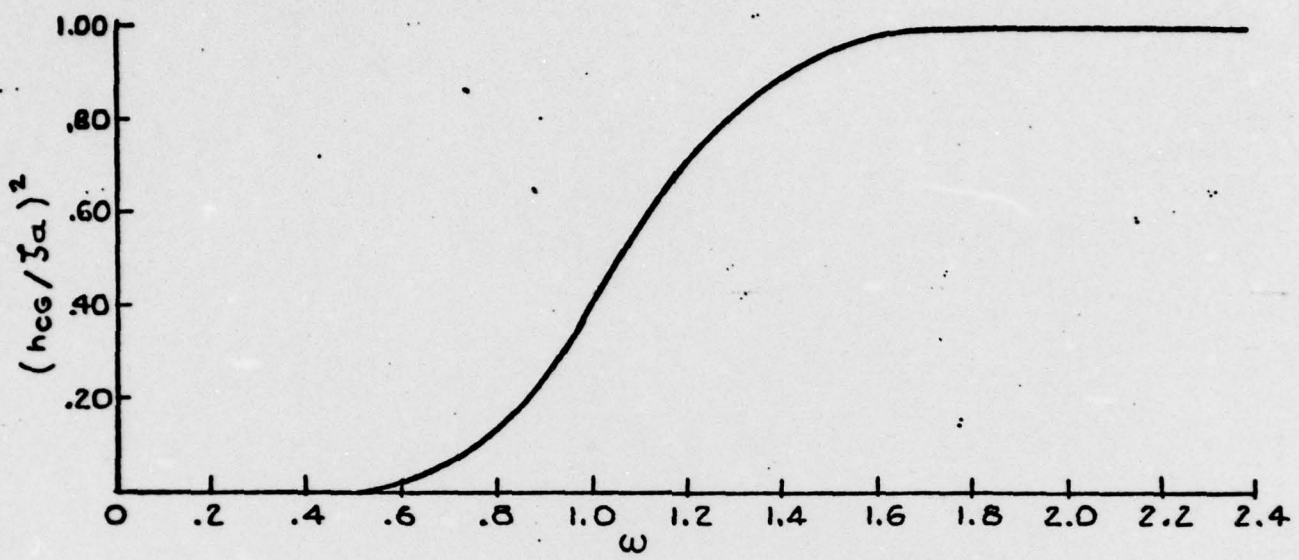
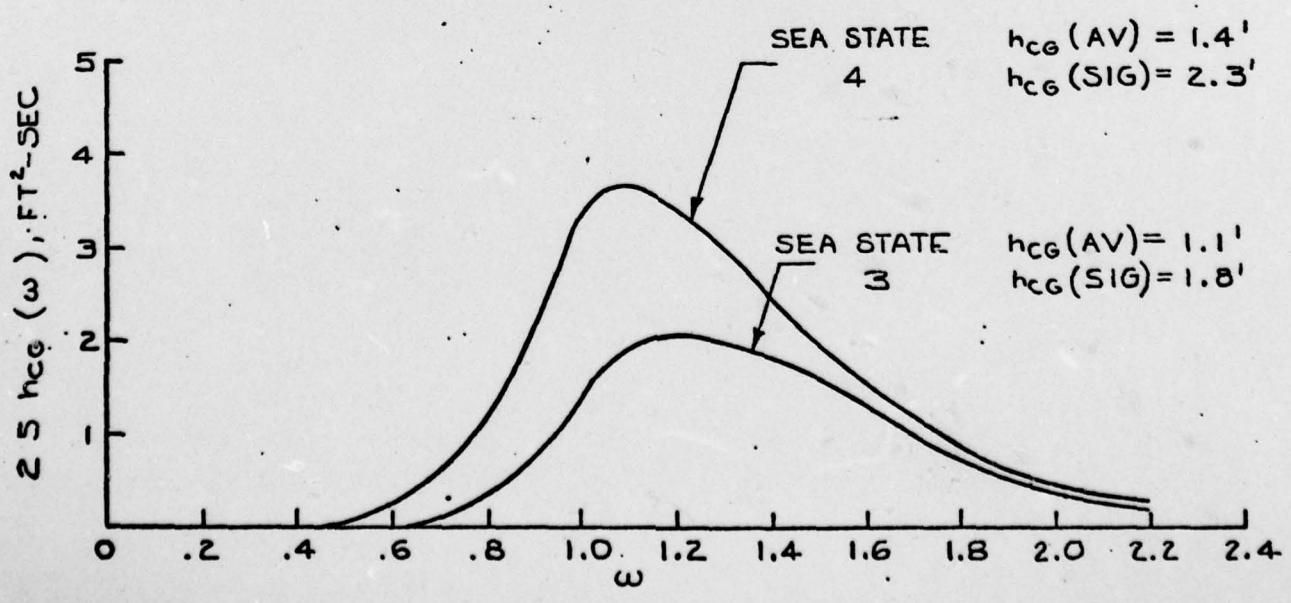


FIGURE 6
 MOTION RESPONSE SPECTRA
 FOR
 RELATIVE MOTION AT CENTER OF GRAVITY



DOCUMENT CONTROL DATA - R & D

(Security classification of title, body of abstract and indexing annotation must be entered when the overall report is classified)

1. ORIGINATING ACTIVITY (Corporate author) Ocean Science and Engineering, Incorporated		2a. REPORT SECURITY CLASSIFICATION Unclassified	
		2b. GROUP N.A.	
3. REPORT TITLE FLOATING OBJECT RECOVERY STUDY			
4. DESCRIPTIVE NOTES (Type of report and inclusive dates) FINAL			
5. AUTHOR(S) (First name, middle initial, last name) RICHARD J. HELGESON			
6. REPORT DATE August 31, 1970		7a. TOTAL NO. OF PAGES 46	7b. NO. OF REFS 12
8a. CONTRACT OR GRANT NO. N00014-69-C-0256		8b. ORIGINATOR'S REPORT NUMBER(S) 11-2003	
8c. PROJECT NO. d.		9a. OTHER REPORT NO(S) (Any other numbers that may be assigned this report) N.A.	
10. DISTRIBUTION STATEMENT Reproduction in whole or part is permitted for any purpose of the United States Government.			
11. SUPPLEMENTARY NOTES N.A.		12. SPONSORING MILITARY ACTIVITY Office of Naval Research	
13. ABSTRACT <p>A study was conducted to determine a method to recover floating objects from the surface of the ocean. Model test tank investigations conducted at Stevens Institute of generating a localized flow field which would refract waves were investigated for a possible practical application. Several methods of generating a localized flow field in the open ocean were investigated. The flow field could attenuate wave energies in an area which could possibly facilitate the recovery of floating objects from the ocean surface.</p>			

